Laboratory Manual

Characterization of Materials (MS604A)

Materials Science Programme

Indian Institute of Technology, Kanpur

LIST OF EXPERIMENTS

1. Microstructures

Object

Study of microstructures of metals and alloys after various phase transformations.

Theory

The nature of phase transformation has a profound influence on the microstructure of a material. This can be demonstrated by observing the following structures formed on solidification, or solid state transformation.

1. Solidification

(a) Pure metal

When a melt is poured into a container which is at a much lower temperature than the melt, large undercooling occurs in the regions where the melt comes into contact with the container walls. The liquid is cooled well below its freezing temperature and the nucleation of the solid phase occurs adjacent to the walls. The formation of these solid crystals releases the latent heat of fusion and the degree of supercooling is reduced in liquid adjacent to these crystals. Consequently no fresh nuclei form in the center of the mold, and the growth of the crystals formed near the mold wall continues inwards. The direction of growth of the crystals is opposite to the direction of heat flow from the centre of the ingot to the container walls. This results in long columnar crystals perpendicular to the walls (Fig. 1.1).

Figure 1.1 Long columnar grains

(b) Solid solution

When two or more elements combine in such a way that the elements are mixed on an atomic scale, the product is called a solution. In solid state it is called a solid solution. Every solid solution is single phase. Solid solution may be primary or secondary. Primary solid solutions have the crystal structure of one of the elements in the system, and can be thought of as a solution of the other element or elements in that element. The host element is called solvent, the other elements is solute. Primary solid solutions may contain any percentage of solute from zero to some maximum percentage which is called the solubility limit. If the solid solution phase exists

between two solute concentrations neither of which is zero, then it is a secondary solid solution. Unlike pure metals, solid solutions generally freeze over a range of temperature. During solidification of an alloy, this feature introduces compositional inhomogeneity, which is reflected in the microstructure. The chemical inhomogeneity comes about in the following way. In an equilibrium diagram the field between the liquids (X-Y in fig. 2.2) and solidus (X-Z) represents the temperature range in which solidification occurs. If an alloy of composition C is cooled from the molten state, the freezing starts at temperature T_1 when the first solid to form is of C_1 composition. It can be seen that the crystals are richer in A than the original melt. The remaining melt is consequently richer in B than the original liquid. As the temperature decreases, the composition of newly formed solid phase and the melt change. At a temperature T_2, for example, the compositions of the solid phase and the liquid phase are indicated by C_2 and C_3. Thus the composition of the solid phase becomes progressively richer in B.

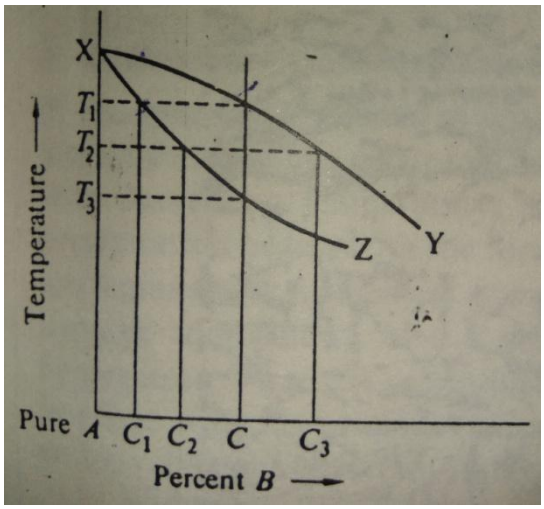

Figure 1.2 An equilibrium diagram indicating the composition of solid and liquid phases during solidification of an alloy

The microstructural effect arise because the liquid phase enriched in B has a lower freezing temperature and this results in a different pattern of supercooling. The initial stage of solidification of an alloy is similar to that for a pure metal. During the period of columnar growth, however, the solid phase develops protuberances. This is because the solute atoms of B are rejected during the formation of the solid phase and the liquid in the immediate vicinity of the solid-liquid interface is enriched with B. this liquid has lower freezing temperature. Since the interface can be assumed to be at equilibrium and the actual temperature gradients quite small, the liquid ahead of the interface is supercooled and the supercooling increases with the distance from the interface. As a result, any solid protuberance ahead of the plane interface grows more rapidly than the plane interface since the liquid solidifies more readily with increased supercooing. A dendritic pattern of growth is thus obtained.

Specimens

(i) Pure Metal: e.g., zinc, sand cast
Etchant: 50 per cent HCL
Microstructure: Long columnar grains (Fig.1-1)

(ii) Solid Solution: e.g., Cu/30 Wt per cent Zn alloy, sand cast.

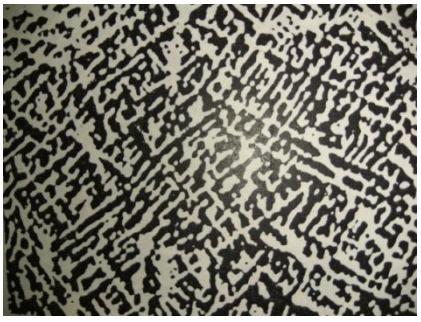

Figure 1.3 Dendritic structure in a polycrystalline specimen

Etchant: 5 g $FeCl_3$, 96 cc C_2H_5OH, 2 cc HCL (alcoholic ferric chloride solution).
Microstructure: A dark skeleton pattern is observed inside the columnar grains (Dendritic structure) (Fig. 1.3).

(c) Two-phase structures

(i) Eutectic Structures

In Eutectic reaction a liquid phase transforms in to a mixture of two solid phases with different compositions and crystal structures

Liquid → α +β

On cooling, the melt with composition C in Fig. 1.4 forms a two-phase microstructure with crystals of α and β. The initial formation of an α crystals causes the surrounding liquid to be supersaturated in β with the result that the conditions are favourable for the nucleation and growth of β crystal next to the α crystal already formed.

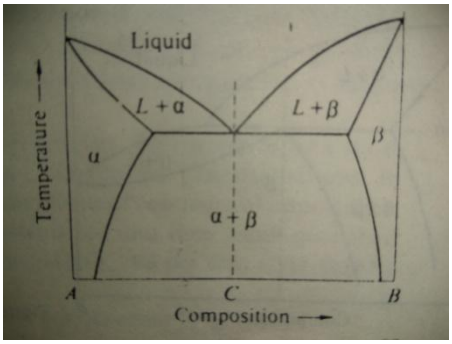

Figure 1.4 Binary eutectic system

Specimens: e.g., Cu/8.4 Wt per cent P alloy, sand cast.

Etchant: 10g $FeCl_3$, 30 cc HCL, 120 cc water (aqueous ferric chloride solution)

Microstructure: Grains are composed of colonies of fine eutectic structure.

Figure 1.5 Eutectic structure

Peritectic Structure. In A lamellar pattern consisting of crystals of copper-rich solid solution (dark) and copper phosphide (Cu_3P) (white) is observed (Fig. 1.5)

)

(ii) Peritectic reaction: a solid and a liquid phase react to produce another solid phase.

α + Liquid → β

If the melt with composition C in Fig. 1.6 is cooled below temperature T_p, the product phase β starts to form at the interface between α and liquid. The growth of this phase is dependent on the diffusion of atoms on one side of β to the other side. Since diffusion is slow in solid state, equilibrium microstructures are rarely obtained in peritectic systems.

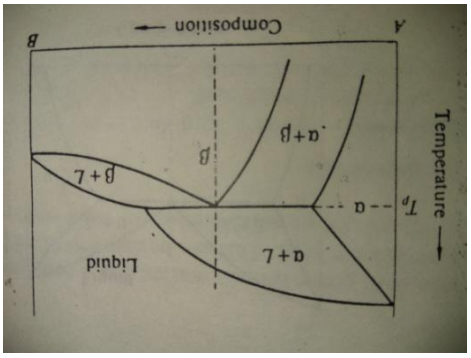

Figure 1.6 Binary peritectic system

Specimen: Cu/37 Wt per cent Zn alloy, sand cast

Etchant: 5g $FeCl_3$, 96cc C_2H_5OH, 2 cc HCL (alcoholic ferric chloride solution).

Microstructure: Crystals of copper-rich solid solution (light etching), partly surrounded by β crystals (dark), are observed. B crystals have formed by a peritectic reaction (Fig. 1.7).

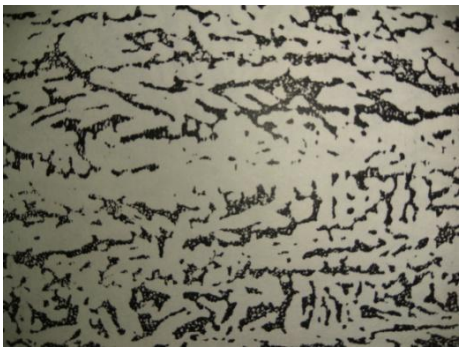

Figure 1.7 Dark crystals of beta phase have formed by a peritectic reaction

2. Solid state transformation

In alloy systems every change of temperature causes a change in the relative free energies of the possible phases. Therefore a change in temperature can bring about replacement of existing phases by new ones provided this will reduce the free energy of the system. Such transformations usually take place by nucleation and growth. Stable nuclei of the new phase form and then grow into the parent phase. Growth of the new phase can occur either by a diffusional or by a shear mechanism. In diffusional mechanism atoms move independently to positions coherent with the crystal structure of the new phase. If the new phase differs in composition, long-range diffusion must also occur.

When the growth of the new phase occurs by distortion of the parent phase, involving cooperative movement of atoms the phase change is termed a shear (or diffusion-less or martensitic) transformation. The interface is propagated by means of the systematic shear of region of the parent phase in such a way as to create an entirely new lattice.

(a) Diffusional transformations

(i) Precipitation from solid solution.

Precipitation of a solute-rich phase from a solid solution can occur in an alloy system if the solubility limit decreases with decreasing temperature, which is usually the case. The process of precipitation begins with the formation of aggregates of solute atoms, which are regions with a chemical composition different (richer in solute) from the average composition of the solid solution. As the ageing proceeds, the aggregates grow and then produce precipitates which generally have a definite interface with the matrix; the crystal structure of the precipitates may be entirely different from the matrix.

Widmanstatten patterns are formed if the precipitation occurs along certain crystallographic planes of the parent phase. This can happen when the growth of precipitates along these planes is favoured on account of good atomic matching across the precipitate/matrix interface resulting in lower interfacial energy. Some alloys in which precipitation occurs are Al-Cu, Cu-Bi, Ni-Ti, Fe-N.

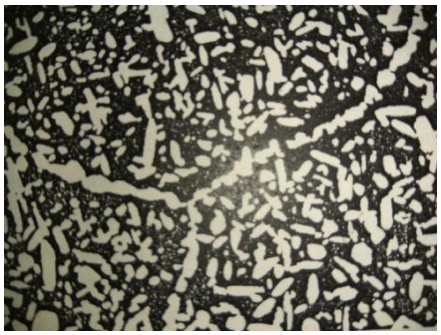

Figure 1.8 Light etching precipitates of α phase in β matrix. Precipitates on three grain boundaries are also observed

Specimen: e.g., Cu/40Wt per cent Zn alloy; homogenized at 850^0C, quenched, and then aged at 700^0C for 1 hr.

Etchant: 5 g $FeCl_3$, 96 cc C_2H_5OH, 2 cc HCL (Alcoholic ferric chloride solution).

Microstructure: A finally dispersed precipitation of α phase is observed within the grains and on the grain boundaries. (Fig.1.8)

(ii) Eutectoid transformation.

In eutectoid reaction, a single solid phase transforms into two new phase on cooling.

$\alpha \rightarrow \beta + \gamma$

The two phases that are formed both have different compositions and structures from the parent phase. The compositional changes have to be brought about entirely by slow process of long-rang diffusion in solid state. During their growth, the constituent phases are often in the form of alternate lamellae behind a common incoherent interface with the parent phase.

Alloys such as Fe-C and Cu-Sn undergo eutectoid decomposition.

Specimen: e.g., 0.8 per cent carbon steel, austenitized and then slowly cooled.
Etchant: 2 per cent Nital (2 per cent cons. HNO_3, 98 per cent C_2H_5OH by volume)
Microstructure: A fine lamellar structure of ferrite and cementite is observed.
This aggregate is known as pearlite. (Fig. 1.9)

Figure 1.8 Pearlitic structure. Lamellar aggregate of ferrite and cementite

(b) Diffusionless (martensitic) transformation

The martensitic transformation occurs by a shear mechanism without a change in composition. The atomic movements that occur during this transformation are less than an interatomic distance. Due to shear mechanism, the shape of the transformation region is changed. Hence there is an increase in strain energy of the system. To minimize the strain energy, the new phase generally forms as thin plates.

Alloys such as Fe-C, Cu-Zn, In-Tl and Au-Cd transform by a shear mechanism under suitable conditions. Martensitic transformation in steel have been used to develop numerous alloys of commercial importance.

Figure 1.10 Thin plates of martensite

Specimen: 0.4 per cent carbon steel, austenitized and then water quenched

Etchant: 2 per cent Nital (2 per cent conc. HNO_3, 98 per cent C_2H_5OH by volume)

Microstructure: Thin plates of martensite are observed (Fig. 1.10)

Experimental procedure

Equipment required

(i) Polished specimens with known history: zinc, sand cast ; Cu/30 Wt per cent Zn alloy, sand cast ; Cu/8.4 Wt per cent P alloy, sand cast ; Cu/37 Wt per cent Zn alloy, sand cast ; Cu/40 Wt per cent Zn alloy, homogenized, quenched, and aged; 0.8 Wt per cent C carbon steel, austenitized and slowly cooled; 0.4 Wt per cent C steel, austenitized and water quenched; others may be added or substituted.

(ii) Metallurgical microscopes, magnification up to 1000x

(iii) specimens with unknown history.

Procedure

Specimens showing various phase transformations have already been polished. Fix the specimens on glass slides by means of Plasticine and level the etched surface with the help of an available levelling device. Or put them directly if using inverted microscope. Examine the microstructure. Also polish and examine the structure of the given unknown specimens.

Questions

1. State what you can about the history of the given unknown specimens.
2. What will be the effect of the rate of cooling on the interlamellar spacing in pearlite?
3. Will the eutectic or peritectoid transformation undergo completion at a more rapid rate? Explain.
4. Can you determine habit planes of the precipitates with optical microscopy?
5. Why are the regions near grain boundaries free of precipates in the specimen of Cu/40 Wt per cent Zn alloy examined by you?

References

Prof. E. C. Subbarao, Prof. L.K. Singhal, Prof. D. Chakravorty and Prof. Marshal F. Merriam, “Experiments in Materials Science” Tata Mcgraw-Hill Publishing Co. Ltd.

2. Hall Experiment

Introduction

When a rectangle parallepiped semiconductor conductor is placed in a magnetic field (Held perpendicular to the direction of the current), a voltage is developed across the specimen in the direction perpendicular to both the current and the magnetic field (Fig.1). It emerges because the moving charges are deflected to one side by the magnetic field. The charges accumulate on a face of the specimen until the electric field associated with the accumulated charges is large enough to cancel the force exerted by the magnetic field. This corresponds to the steady state condition for that value of the applied magnetic field. We are concerned only with the steady state condition.

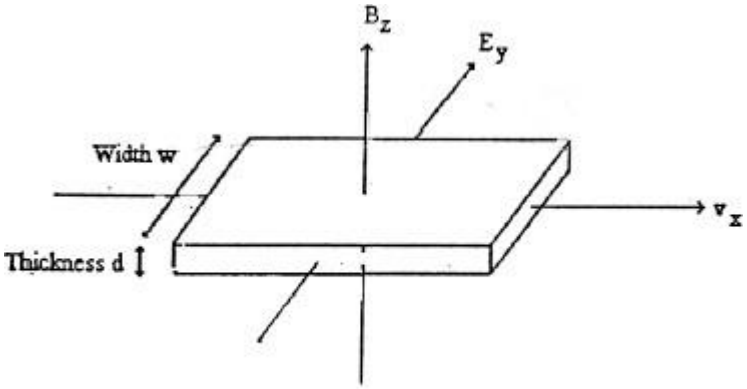

Fig. 1

The Lorentz force on a carrier of charge e and drift velocity **v** in a magnetic field of intensity **B** is given by

$$\mathbf{F} = e\,(\mathbf{v} * \mathbf{B}) \quad \text{.....(1)}$$

and perpendicular to both **v** and **B**.

Thus charge carriers get deflected in the negative y direction (fig. 1), get accumulated on the x-z face and generate a Hall field $\mathbf{E}_y$ along the width (i.e, y direction) of the semi conductor. This field repels the movement of charge carriers. That means the force (eE) caused by the Hall field opposes the Lorentz force. In a steady state situation, the force (eE) balances the Lorentz force such that

$$e\,E_y = e(v_x\,B_z) \quad \text{..... (2)}$$

But $E_y = V_H / w$ ..... (3)

where V_H is the Hall voltage and w is the width of the semi conductor. Also v_x is related to the current I_x flowing in the x-direction such that

$I_x = n\ e\ v_x\ A$ .....(4)

Where n is the number of charge carriers per unit volume and A (= wd; d being the thickness) is the cross sectional area.

Combining equations (2), (3) & (4) we get

$V_H = (I_x\ B_z) / (n\ e\ d)$ ..... (5)

Or, $V_H = (I_x\ B_z\ R_H) / d$ ..... (6)

If $R_H = 1/(n\ e)$ .....(7)

The parameter R_H is called the Hall coefficient. Thus measurement of the Hall voltage can give the concentration of charge carriers. Also the sign of Hall voltage can determine the nature of charge carriers (Think it over!).

In practice, misalignment and thermal voltages are usually appears when the sample current exists but no magnetic field. A, and B in Fig. 2 represents the probe for measuring the Hall voltage. With no magnetic field applied, the equipotentials are the lines approximately perpendicular to the lines of current flow. If A and B are not on the same equipotential, an additional voltage will be measured between them due to ohmic resistance, giving a constant error to the Hall voltage measured. However, this misalignment voltage is small and its effect could be minimized by reversing the magnetic field. Similarly the error due to thermally generated voltage (I^2R heating) could be minimized by reversing the sample current.

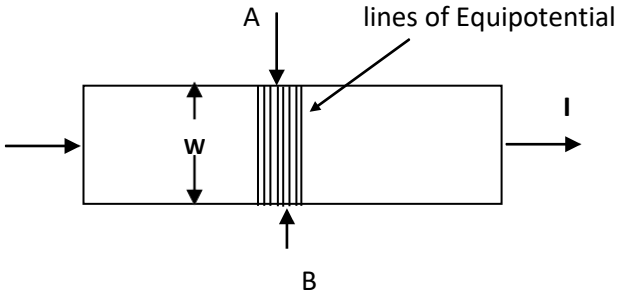

Fig. 2

Experimental Setup and measurement

The sample is a lightly doped (n or p type) Ge crystal of thickness 0.5 mm. It is fixed against a strip of Bakelite by four spring type pressure contacts. The current and voltage leads are clearly defined by green and red colour respectively. Check the connections before applying the current, which should not exceed the limit of 5 mA to avoid any damage of the sample. Make the, connection as shown in Fig. 3. The direction of current and magnetic field can be reversed by interchanging the respective banana pins.

Repeat the measurement by

(a) reversing the current in the semi conductor,

(b) reversing the magnetic field, and

(c) reversing both the current and the magnetic field.

The corresponding values of Hall voltages are designated as $V_h(B, I)$, $V_h(B, -I)$, $V_h(-B, I)$ and $V_h(-B, -I)$ respectively.

Hall voltage is finally given by:

$$V_H = 1/4 [\{V_H(B, I) – V_H(B, -I)\}-\{V_H(-B, I)- V_H(-B, -I)\}]$$

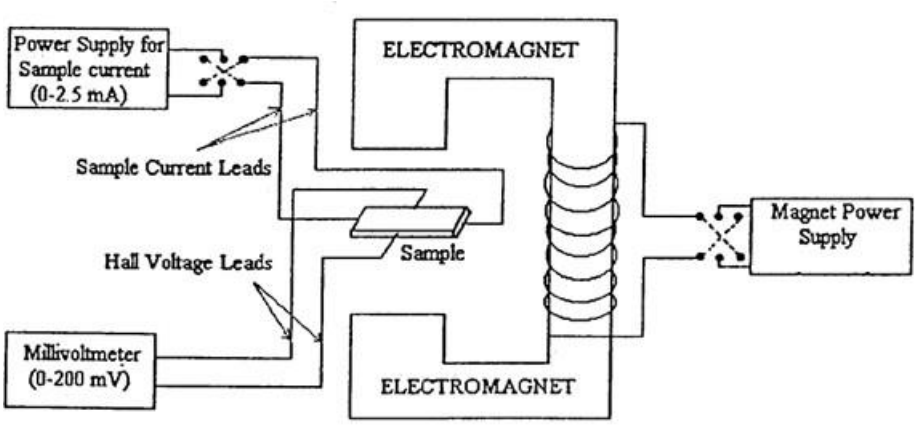

Fig. 3

Such measurement is to be repeated with another current setting (I) in the range 1-5 mA. Also note down the direction of current in the semiconductor piece. Make a schematic diagram showing the semiconductor crystal and directions of current, magnetic field and Hall voltage (V_H) measured with sign for all the four situations.

Do the following

1) Plot Hall voltage (V_H) as a function of magnetic field (B) for each setting of current in the semiconductor.
2) Use eqn. (5) to find out the value of Hall coefficient R_H. Is there a better way to determine R_H? (Hint: Graphical method)
3) Determine the concentration of charge carriers from the data obtained.
4) Find out the nature of the charge carriers.

Questions:

1) What do you understand by the term mobility? How will you determine its value? Given $\rho = 7\ \Omega$cm for n type and $\rho = 10\ \Omega$cm for p type Ge crystal.
2) What is the physical significance of Hall coefficient (R_H)?
3) What is the direction of Lorentz force for electrons and holes? Justify your answer.

References

1. C.Kittel, "Introduction to Solid State Physics".

2. W. Angrist, Scientific American, 205, 124 (1961).

3. EJM.Putley, “The Hall Effect and Related Phenomena", Butterworths, London (1960), p.2.

3. Electrical resistivity and band gap of semiconductor

Objective

To determine the energy band gap of a given semiconductor by measuring its electrical resistivity as a function of temperature by a four probe method.

Set up

It consist of

(1) A semiconductor crystal piece mounted on a non conducting bottom surface is placed under four spring loaded contact probes spaced equally.

Dimensions are

Sample thickness (w): 0.5mm,

Probe separation (s): 2mm

(2) Oven with a thermocouple

(3) PID temperature controller with display.

(4) Constant current source.

(5) Microvolt meter.

Procedure

(1) Gently remove the sample holder out the oven and carefully check the sample position, contacts of the leads, separation between the leads and the thickness of the sample.

(2) Identify the voltage and the current leads.

(3) Having placed the sample holder inside the oven, switch on the current source and the voltmeter.

(4) Set a constant current (e.g. 5 mA) to flow through two outer probes and turn on the oven power supply. The sample heating begins automatically with temperature indication on the display. Measure the voltage drop across the middle two probes at the temperature interval of ~ 5°C up to 180°C

Result

Calculate the electrical resistivity (ρ_0) using the relation:

$$\rho_0 = \frac{V}{I} \times 2\pi s$$

where 's' is the probe separation.

Use ρ_0 to determine the electrical resistivity ρ from relation

$$\rho_0 = \frac{\rho_0}{G}$$

where G is a function dependent on the (W/S) ratio and known as correction factor when measurements are carried out on a thin slice non conducting bottom.
Take the value of 'G' as 6

Plot ln ρ Vs $\frac{1000}{T}$ curve and find out the energy band gap (E_g) of the semiconductor.

The electrical resistivity follows the relation

$$\rho = A\, exp\frac{E_g}{2kT}$$

where A is the pre-exponential factor and 'k' is the Boltzman constant.

Questions

(1) Why is four probe method is preferred over two probe measurement system? Discuss briefly.
(2) Can you measure resistivity of the material by this technique placed on a conducting surface?
(3) How you measure the activation energy and band gap of an extrinsic semiconductor by this method?
(4) Can you determine the band gap of the material by measuring the resistivity at low temperatures? What temperature range you think as most appropriate to measure the band gap of the material you worked on.

4. Dielectric behaviour of Barium Titanate

Object

To study the dielectric behaviour of ceramic barium titanate through the tetragonal-cubic transformation

Theory

Barium titanate (BaTiO3) exhibits the following polymorphic transformations:

Rhombohedral : Orthorhombic : Tetragonal : Cubic
-80^0C 0^0C 120^0C

The tetragonal cubic phase change at 120˚C is studied in the present experiment. The cubic $BaTiO_3$, stable at temperatures over 120˚C, has the perovskite structure (Fig. 1). On cooling below 120˚C, one of the cubic edges becomes elongated so that the material assumes tetragonal symmetry ($a=b\neq c$; $\alpha=\beta=Y=90°$). At room temperature, $c/a=1.01$; i.e. the c axis is elongated by 1%. The titanium ion is centrally located with respect to the six surrounding oxygen ions in the cubic phase. The equidistant tetragonal distortion produces a perturbation in the crystalline potential within the unit cell so that the titanium ion, instead of remaining equidistant from the two oxygen ions in the c direction, moves closer to one oxygen ion or another. This non-centrosymmetric location of the titanium ion sets up a permanent dipole and cause spontaneous ionic polarization. When the direction of the spontaneous ionic polarization of a material can be reversed by an applied electric field, the material is called a ferroelectric and the phenomenon, ferroelectricity. A ferroelectric material (e.g. $BaTiO_3$) exhibits the following characteristics:

1. High dielectric constant, 10 - 10000 compared to 1-10 for most materials.
2. A hysteresis loop between the dielectric displacement, D and the electric field E analogous to the B-H hysteresis loop of a ferromagnetic material .
3. A critical temperature called the Curie temperature, beyond which the spontaneous polarization is lost and the material becomes paraelectric.
4. A sharp peak in the dielectric constant – temperature plot, occurring at the Curie temperature.
5. Domains or volume elements in which the direction of polarization is uniform.

6. Domain growth: under the influence of an applied electric field, favourably oriented domains grow at the expense of those less favourably oriented, through domain wall motions.
7. Curie – Weiss temperature dependence: above the Curie temperature, the dielectric constant (ϵ) varies with temperature (T) as stated in the Curie -Weiss law.

   $\epsilon = C / (T-Tc)$ ---------- (1)

   Where C is called the Curie constant and Tc is the curie- Weiss temperature.

8. Piezoelectricity: electric charge is generated by the application of mechanical pressure and conversely, crystal dimensions can be changed by applying an electric field. The chief application of ferroelectric materials such as $BaTiO_3$ arise from these properties . for example, ferroelectric materials are used for miniature capacitors because of their high dielectric constant ; for memory devises because of their D-E hysteresis loop ; or for electrochemical transducers because of their piezoelectric behavior.

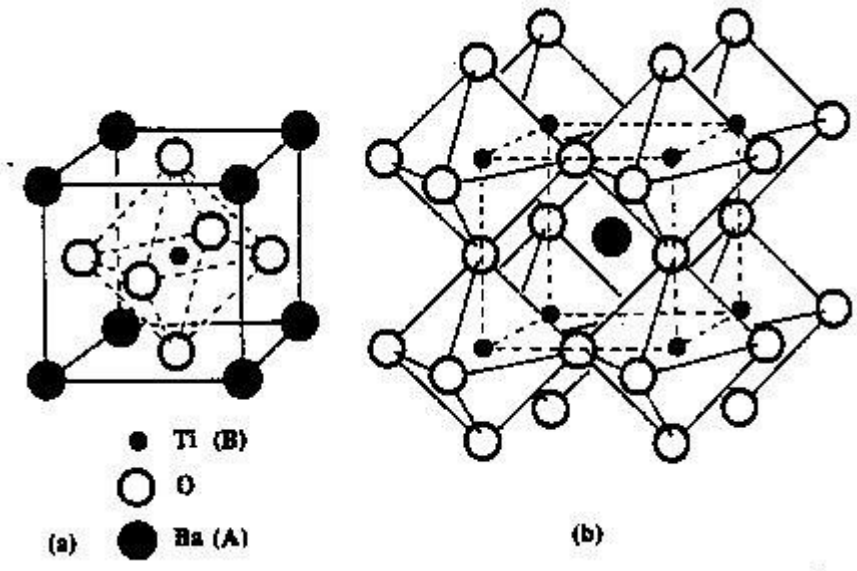

Fig. 1 Ideal perovskite lattice of cubic $BaTiO_3$
(a) One unit cell (b) The linking of the TiO_3 octahedra through corners in a three dimensional framework.

Equipment

Electroded ceramic disk of barium titanate, Micrometer, Sample holder, A tube furnace, Chromel-alumel thermocouple and Temperature controller (or Variac and potentiometer), Capacitance bridge, such as general radio impedance bridge type 1650 A or LCR meter.

Procedure

(1) Measure the diameter and the thickness of the specimen with a micrometer.

(2) Place the sample disk in the specimen holder, and the specimen holder in the tube furnace.

(3) Connect the specimen holder to the LCR meter.

(4) Measure capacitance and dissipation factor at a frequency of 1kc/s at room temperature and at every 1-2°C intervals up to 150°C. Keep the rate of temperature rise 1-2^{0}C.

(5) Plot:

(i) Capacitance Vs temperature
(ii) Derivative of dielectric constant with respect to temperature (dK/dT vs T).

(6) Repeat the measurement on cooling.

Observations

Tabulate the temperatures, capacitance, relative dielectric constant (ϵ), dissipation factor (tan δ).

Thickness of specimen = 3.5 mm
Diameter of electrode = 11.4 mm
Area of the electrode =

Use the formula

$$e = \frac{C}{C_0} = C\frac{d}{Ae_0} \qquad \text{---------- (2)}$$

Where

C is the measured capacitance, in farads

C_0 is the geometrical capacitance in vacuo
d is the thickness of the capacitor, in meters
A is the electrode area of the capacitor in square meters
ϵ_0 is the permittivity of vacuum (8.854×10^{-12} farad/m).

Questions

(1) Estimate the temperature coefficient of the capacitance in the temperature range normally used for electronic components, say, room temperature to 80°C.

(2) What factors contribute to the different between the observed and the literature value (120°C) of the Curie temperature?

(3) How does the dissipation factor varied in the neighbourhood of the Curie temperature?

(4) Estimate in the energy loss in the capacitor per second at room temperature.

(5) From your data, can you find out the curie constant and the Curie-Weiss temperature? If so how? If not, why?

(6) A 100 pF $BaTiO_3$ capacitor is how much smaller than a Titania capacitor (K' =80)? (Assume the same dielectric strength for both materials and negligible electrode volume).

References: Experiments in Materials Science; Prof. E.C. Subbarao, Prof. L.K. Singhal, Prof. D. Chakravorty, Prof. Marshal F. Marriam, Prof. Raghavan

5. Electrical conductivity of ionic solids

Object

To study the electrical conductivity of polycrystalline sodium chloride

Theory

Electrical conductivity in ionic solids usually arises from the migration of ions under the influence of an electric field. Experiment show that in the alkali halides the positive ions are much more mobile than the negative ones. The mobility of ions in a perfect lattice (a lattice in which all sites are occupied by the proper ions) is extremely low. This is because of the high energy barriers preventing interchange of atoms. Hence, the presence of some lattice defects (viz. vacancies or interstitials) is essential for the occurrence of ionic conductivity. Such defects are indeed present in ionic crystals (and in metals also) and provide a thermodynamically stable state for the solid. The defect concentration is dependent on temperature. Thus, the expression for the concentration of a pair of positive and negative ion vacancies is given by

$n = C \exp(-\phi/2kT)$ ..... (1)

Where,

n is the number of pairs of vacancies
ϕ is the formation energy of such pair
C is a constant
k is the Boltzmann constant
T is temperature in ^{0}K

The positive ions surrounding the positive ion vacancy will have a finite probability of jumping into it. As a result , the vacancy will move through the crystal by virtue of positive ions jumping into it and diffusion (i.e. ion movement without any external field applied) becomes possible. When an electric field applied to the solid, the probabilities of ion jumps in the directions parallel and antiparallel with the field are altered so that there is an effective movement of positive ion vacancies toward the anode. This means that there is a net effective movement of positive charge toward the cathode. The expression of conductivity (σ), derived on this basis is of the following form:

$$\sigma = A\, exp\left[-\frac{(E_m+\frac{\$}{2})}{kT}\right] \quad \text{..... (2)}$$

Where

A is a constant for a particular crystal
E_m is the activation energy for migration

ϕ is the formation energy of such pairs
k is a Boltzmann constant
T is temperature in ^{0}K

Thus, from a plot of **$\log_{10}$ vs 1/T** one can calculate the value of **$(E_m + \phi/2)$**. Plot of this sort for real alkali halides typically have the form of fig.1. There is a break observed somewhere in the temperature range of 300 to 700 degree centigrade depending of the impurity of the crystal. This is known to arise from divalent positive impurities in the crystal. By the electrical neutrality condition, for each divalent positive ion present there must be a positive ion vacancy. Thus at lower temperatures such crystals may contain more positive ion vacancies than would be expected on the basis of thermal equilibrium alone. In fact, below a critical temperature essentially all the vacancies arises because of the divalent impurities. The number thermally generated (eqn.1) becomes insignificantly small. Thus the number of vacancies becomes temperature independent and the temperature dependence of the conductivity is controlled only by the mobility energy E_m. Above this temperature the number of thermally produced vacancies would predominate over the number due to the impurity atoms and consequently the conductivity will depend on the energy $(E_m + \phi/2)$. This means that the slope of $\log_{10}\sigma$ vs 1/T should be E_m and $(E_m + \phi/2)$ respectively in the two temperature ranges. Hence by determining these slopes, the values of E_m and ϕ can be calculated.

Equipment

Tubular furnace,Temperature controllern(ornVariac), LCR meter (or Resistance measuring bridge with an ac signal source and null detector), Alumina crucible (50cc), Polycrystalline NaCl and Silver plates. Specimen holder is shown in fig.2 where Alumina crucible consists of polycrystalline sodium chloride. S1 and S2 are two silver rods act as electrodes and their dimensions inside the crucible are 40 mm long and 18 mm wide. The separation between these electrodes is ….. mm. The electrical lead wires are connected to S1 and S2. T.C. represents the chromel-alumel thermocouple wires.

Procedure

1. Before mounting the specimen assembly as shown in fig 2, crucible is filled with NaCl powder with T.C. embedded in it. The specimen is melted in a furnace at around 815^{0}C. The silver plates S1 and S2 are clamped with a screw after inserting a metallic block between them and then the whole thing is immersed in the molten salt. Some more Nacl powder is added to make a for any loss during melting. When the crucible is cooled, one gets a polycrystalline NaCl specimen with two silver

electrodes and a T.C. inserted in it. The metallic blocs used to align the electrodes can then be removed.

2. The specimen cell is placed inside a tube furnace, the temperature of which is controlled by a chromel- alumel thermocouple.

3. Connect the thermocouple leads to the appropriate port of the temperature controller. If there is a negative rise in the temperature, it shows incorrect polarity and should be reversed.

4. Since the furnace control is much better in the cooling cycle than in the heating cycle, it is advised to heat the furnace to 700 °C and leave it for ½ hour using variac/Temperature controller.

5. Switch on and allow ½ hour (warming up time) to the LCZ meter before starting measurement. Connect the silver electrodes coming out of the furnace (shown in Fig. 2) to the LCZ meter using crocodile clips. Select **Z** (Impedance) & **θ** (power factor angle) using appropriate push buttons of the LCZ meter. Set the level of supply voltage to 0.5 VAC with a frequency 1KHz ($<10^5$Hz).

6. Take readings of the Z and θ at the interval of 5°C with the sample is cooled.

7. Plot **log σ** Vs **1000/T**.

Precaution

As it takes long time for the furnace to come to a stable temperature it is advisable to switch on the heating arrangement two hours in advance. Do not melt the sample by overheating it (Melting point of NaCI = 801°C).

Questions

1. What is the tempreture corresponding to the break in the $\log_{10}$ G vs 1/T plot ?
2. From your data, determine the values of E_m and ϕ in ev.
3. If some $cacl_2$ powder were added to the specimen before melting it, in which direction would you expect the critical temperature to move ?
4. Why is it important to use a.c. in measuring the conductivity?
5. What are the types of defects in alkali halides ? In silver halides? Which type of charge carrier is more mobile in NaCI?
5. What would be the dominant charge carrier in
   (i) NaCI doped with CO_3^{--} ions and (ii) AgBr doped with Cd^{++} ions?

5. If E_a and E_a' are the (overall) activation energies obtained from a log σ vs 1/T and log σT vs 1/T plots respectively, find a relation between E_a, E_a' and kT where T is the average temperature.
6. What is the order of magnitude of the conductivity of your sample at 700°C? How does it compare with the conductivity of copper at room temperature?

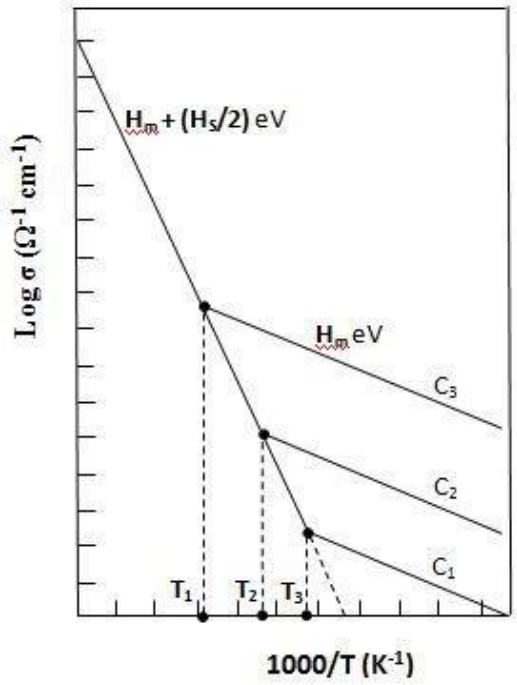

Fig.1: A typical log σ versus 1/T plot for an ionic solid for varying concentrations of aliovalent dopants ($C_1 < C_2 < C_3$). The extrinsic-intrinsic transition (knee) temperature increases as the dopant concentration increases.

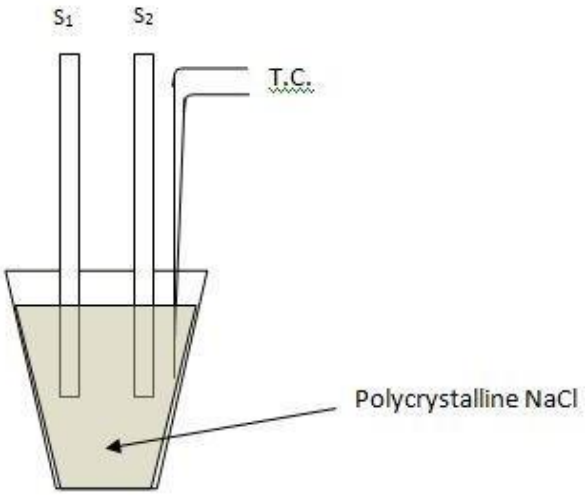

Fig 2: Specimen holder
Useful area of electrode: ..... mm²
Separation between electrodes: ..... mm

References

1 Experiments in Materials Science; Prof. E.C. Subbarao, Prof. L.K. Singhal, Prof. D. Chakravorty, Prof. Marshal F. Marriam, Prof. Raghavan.

6. Thermo-gravimetric analysis (TGA)

Object

To study the stability of the compound and associated changes by measuring its actual weight as a function of temperature

Theory

When a matter is heated, it undergoes certain physical and chemical changes. These physical and chemical changes take place over a wide temperature range. Physical changes such as melting or boiling may occur at widely varying temperatures, depending on the material involved. For example, helium is a liquid at 6K, where as carbon is stable in an inert atmosphere up to 5000K. Chemical changes, such as decomposition or reaction, may also take place at very different temperatures.

The physical and chemical reactions a sample undergoes, when heated are the characteristic of the material being examined. By measuring the temperature at which such reactions occurs and heat involved in the reaction, we can characterize the compounds present in the material. The majority of known inorganic compounds have been so characterized. The physical and chemical changes that take place when an unknown sample is heated provide us the information that enables us to identify the material. These changes also indicate the temperature at which the material in question ceases to stable under normal conditions. This information is very useful to industrial chemists, such as those who make varnishes, paints, and polymers, since it allows them to predict the service lifetime of such compounds.

The analytical procedures that take advantage of these temperature and heat-related properties are thermo gravimetric analysis (TGA), differential thermal analysis (DTA), differential scanning calorimeter (DSC), thermometric titrations (TT), and direct injection enthalpy measurement. Thermo gravimetric analysis (TGA) is concerned with the change of weight of a material as its temperature changes. First, this determines the temperature at which the material losses weight. This loss indicates decomposition or evaporation of the sample. Second the temperature range where no weight loss take place, reveal about the stability of the material. These temperature ranges are physical properties of chemical compounds and can be used for their identification.

Knowledge of temperatures at which a sample is unstable and subject to decomposition or chemical changes is important in the engineering field because it reveals the temperature range over which such materials as polymers, alloys, building materials, packing materials, and high-pressure values may not be used, as well as the temperature at which they may be used safely. It is also important

to analytical chemist, because it helps distinguish samples such as to different polymers or differentiates between a polymer that would fail in service and one that could be satisfactory.

Another important piece of information that can be obtained by TGA is the weight loss by a sample heated to a given temperature. This helps the inorganic or analytical, chemists determine the composition of a compound and follows the reaction involved in its decomposition. It also enables the analytical chemist to identify crystals of unknown composition or determine the percentage of a given compound in a mixture of compounds. For example, if calcium carbonate ($CaCO_3$) is heated to 850^0C, it losses 44% of its weight. Also, the gas evolved can be collected and identified as CO_2. This observation virtually confirms that the reaction

$$CaCO_3 \longrightarrow CaO + CO_2$$

takes place at this temperature. The loss of CO_2 would also lead to a loss in weight of 44%, and the products of the reaction can be identified as CaO and CO_2. The formation of CO_2 can be verified by injecting the off coming gases into a mass spectrometer confirming by the spectrum observed.

Set-up

It consists of

1) A cylindrical furnace fixed on a stand in vertical position,
2) A power supply for the furnace,
3) A temperature controller with a chromel-alumel thermocouple,
4) An electronic balance, ER-100 A

Procedure

A known amount (W grams) of magnesium oxalate $Mg(COO)_2.2H_2O$ (molecular weight 148.36) is taken in a cleaned alumina crucible which, in turn, is allowed to hang freely in position (i.e., in the middle of the heating zone of the cylindrical furnace) from the balance through a platinum wire. The furnace is programmed such that the rise in temperature is at the rate of say, 5°C/minute. While the weight of the sample (with hanging wire and crucible) is directly read on the balance, the temperature is noted from the display mounted on the power supply which reads the temperature of the centralized heating zone. For more accuracy a separate thermocouple (chromel-alumel) can be positioned near crucible and its output are connected to the temperature controller. The temperature can be read directly using a toggle switch provided on the back side of the temperature

controller. The actual weight is then monitored as a function of temperature in the given range, here from room temperature to 550°C.

The following plots are then made from the data obtained

a) Actual sample weight (W) versus temperature (T)
b) Weight difference (ΔW) versus temperature (T)
c) -d (ΔW) / dT versus temperature (T)

Observations and interpretation

1. The plots are observed very carefully and characteristic features noted.

2. The plots are used to determine the range(s) of temperature over which there is
   (i) No change in weight and (ii) weight loss takes place.

3. Also, temperature(s) is (are) determined at which maxima – minima occur(s) in plot c) above.

4. All the results are then reported in the tabulated form.

Discussions and questions

1. Comment on the stability of the compound in different temperature ranges and write down the possible reactions taking place.
2. Estimate theoretically the MgO content in your initial sample and compare the actual weight of the sample at 500°C. Explain and justify your findings.
3. What do you understand by the plot c)? Discuss briefly.
4. If the compound reacts with the environment species at some temperature interval, do you expect weight to increase or decrease? Justify your answer.
5. Assuming that on heating the magnesium hydroxide the following reaction occurs

   $Mg(OH)_2 = MgO + H_2O$

   Estimate the percentage amount of MgO formed in this reaction.
6. MgO is prone to hydration even at room temperature. Can you suggest a way out to make it hydration resistant? (Use literature and/or internet to answer)

7. Thermal analysis of a Pb-Sn alloy

Theory

If a single component system is cooled from the liquid state, it follows from the phase rule that the temperature of the sample undergoing transformation should remain constant during the phase change (Fig.1). It can similarly be deduced that if only two phases are in equilibrium in a binary alloy, the phase change can occur over a temperature range (Fig. 2). When three phases are in equilibrium in a binary alloy, it follows from the phase rule (Eq. 1) that the degree of freedom is zero. The temperature of the material must therefore remain constant during the transformation. When three phases coexist in eutectic composition the alloy solidifies at a constant temperature.

$P+F = C+1$ …… (1)

Where P is the number of phases, F is the degree of freedom and C is the number of components of the system.

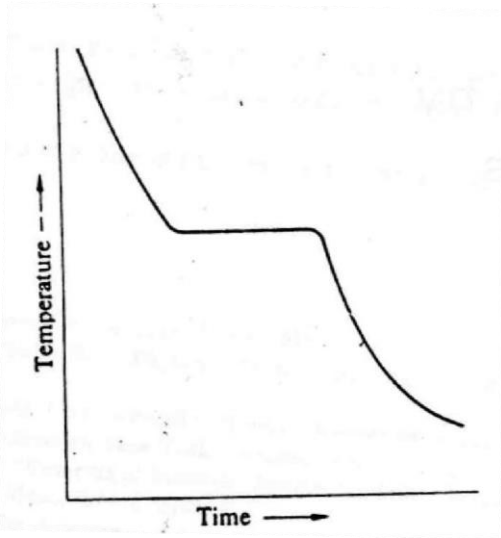

Fig. 1 (a) Cooling curve for a single-component

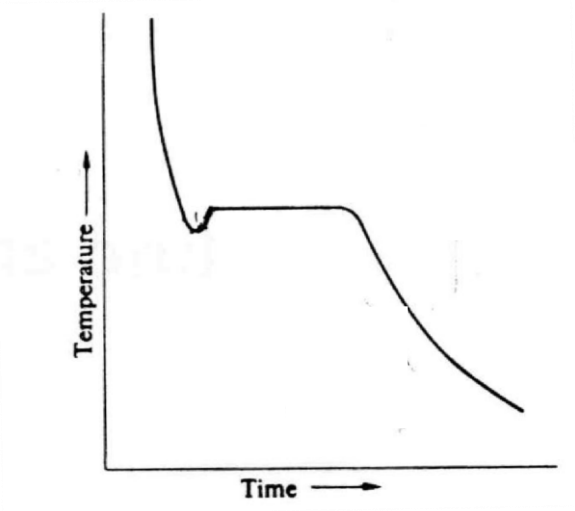

Fig. 1 (b) Cooling curve for a single component system exhibiting super cooling

Under equilibrium conditions, the temperature at which or the temperature range over which a given structural change occurs for a given material is characteristic for that material. Therefore, in thermal analysis, a specimen is heated or cooled and the transformation temperatures are obtained from the points at which changes in slope occur in the heating or cooling curves. Usually the arrest points for plotting equilibrium diagrams are obtained from the cooling curves. Cooling curves offer the advantage of stirring and homogenization of the liquid. However, on account of the

difficulty in the nucleation of the solid phase, the liquid gets cooled below its true freezing point before crystallization begins. This phenomenon, which is known as supercooling, results in an arrest point of the type shown in Fig.1b. The freezing point for the metal is given by the horizontal portion of the curve. When the extent of the supercooling is large, use of heating curves may be preferred.

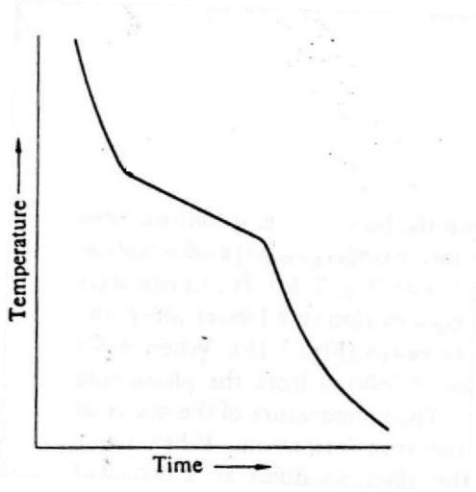

Fig.2: Cooling curve for a binary alloy

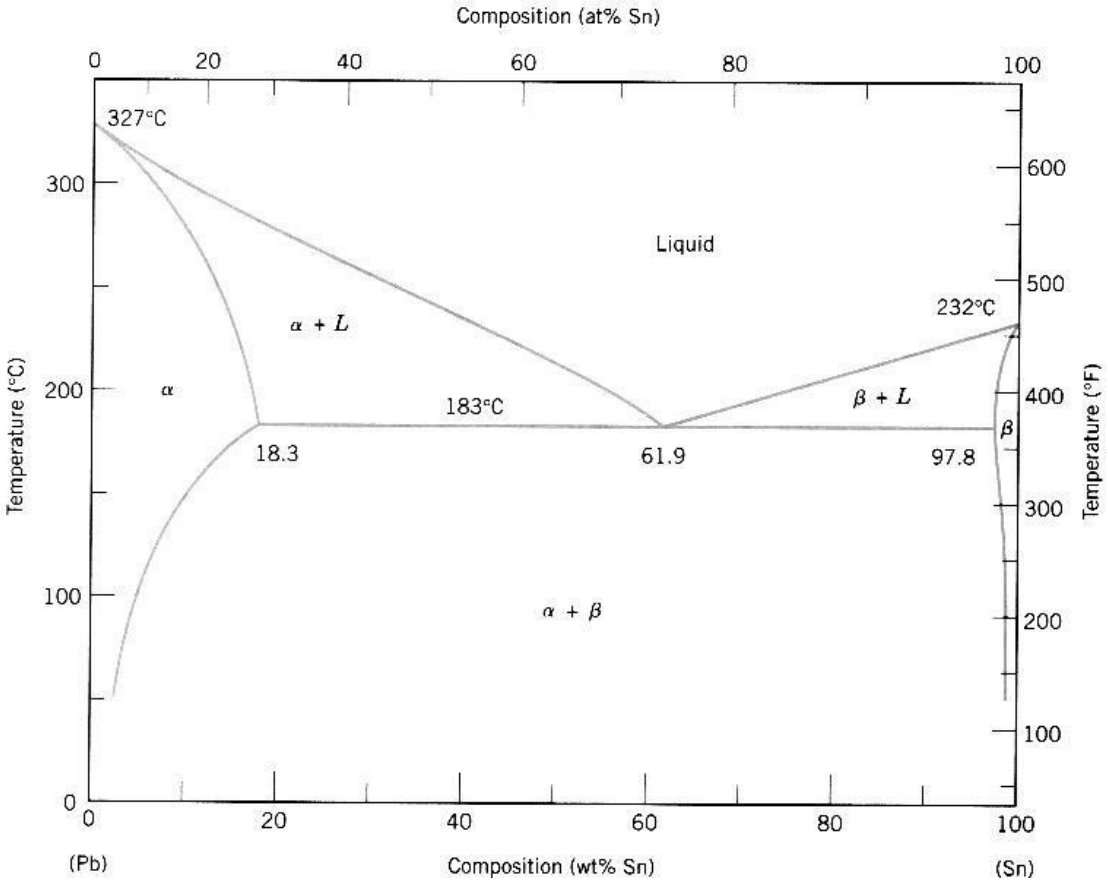

Fig. 3: Equilibrium diagram for Pb-Sn alloy system.

In practice, curves with sharp beginning and end of the transformation are not obtained. The rounding in the curves at the beginning of the reaction is caused by a lag in temperature between the thermocouple and the specimen and also by temperature gradients within the specimen. Therefore the rate of heating or cooling should be small enough to avoid excessive temperature gradients. A satisfactory rate for this experiment is ~1-2^{0}C per minute.

Equipment

A vertical tubular furnace with programmable temperature controller, chromel-alumel thermocouple covered with a protective and insulating sheath, alumina crucible for putting the sample and Pb-Sn alloy of different composition.

Procedure

You have to plot the direct cooling curve for the samples.

1. The alloy containing crucible is kept in the centre of the furnace with chromel-alumel thermocouple attached.
2. The current through the furnace is adjusted to a heating rate of 3-5 ^{0}C per minute.
3. On reaching a temperature ~ 350^{0}C furnace current is switched off and sample is allowed to cool.
4. Temperature readings are taken after every ½ minute with the help of either a temperature controller or a voltmeter connected to the thermocouple and converted into temperature by means of a standard chart for thermocouple (see Table E-5). Be sure that you make any necessary reference junction corrections if converting the mV into temperature.

Observations

1. Record readings after every ½ minute interval as follows

Time	Temperature

2. Plot a direct cooling curve (T versus t) and note the arrest points.
3. Plot ($-\Delta T/\Delta t$) versus t.

Questions

1. Why do you see a plateau region in T versus t plot? Does it give you some idea about the alloy?
2. Account for the dip at the beginning of the plateau region.
3. Use the nature of the T versus t curve to suggest the composition of the Pb-Sn alloy.
4. Plot T versus t curve for the binary alloy at eutectic and other compositions (hypo and hyper eutectic). Compare your curves with those plotted. Justify your results.
5. Use equilibrium diagram of Pb-Sn system to determine the composition of your sample alloys in each case.
6. What type of binary system is represented by the Pb-Sn diagram (Fig.3)?
7. Would you expect a difference in the arrest points obtained by heating curves and cooling curves?

References

1. Chalmers B, and A.G.Quarrell "The physical Examination of Metals," Edward Arnold, London, 1960, Chapter 3.
2. Cherepin V.T. and A.K. Mallik "Experimental Techniques in Physical Metallurgy," Asia Publishing House, New York, 1966, Chapter 5.

8. Annealing effects on microstructure and quantitative metallography

Object

To study the effect of cold working and annealing temperature on microstructure and hardness of commercial copper samples

Theory

A small part of energy consumed in plastic deformation remains stored in the material as an additional internal energy. This increment is associated with lattice defects (such as vacancies, interstitials, dislocations, and stacking faults) generated during the deformation process. The distribution of dislocations is very inhomogeneous. The bulk consists of relatively strain free regions/cells where the dislocation density is low, separated by boundary having dislocations arranged in tightly packed tangles. There may be many such cells in each grain. If deformation occurs at low temperatures, dislocation tangles are retained in the material. The process of recovery and recrystallization can therefore occur during heating or thermally activated processes leading to repair of the structural damage caused by mechanical deformation.

Recovery involves changes in the number and distribution of point defects and dislocations. At low temperatures this is generally caused by the clustering of point defects like vacancies and interstitials, and migration of point defects to dislocations, grain boundaries, and external surfaces. At sufficiently high temperature, the dislocation may eventually gain appreciable mobility and move by both glide and climb to relieve the internal strains. The tangled dislocations in the walls of the cells which formed during deformation, rearrange themselves. The dislocations climb out of their slip planes with the aid of vacancies, (Fig. 1) and some dislocations of opposite sign annihilate each other. The cell wall become more clearly defined and is called sub-boundaries. Throughout this process the dislocation density in the interior of the cell decreases. During the later stages of recovery, the cells increase slightly in size. Small changes in hardness, which are sometimes observed during recovery, can be due to decrease in dislocation and point defect density and to growth of subgrains.

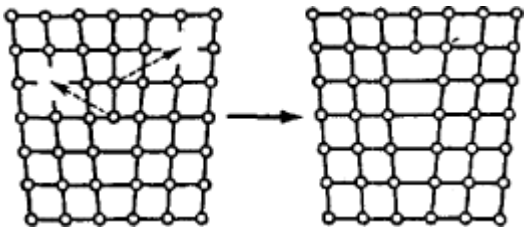

Figure1: Climb of an edge dislocation. Atoms of the extra plane migrate to the vacant lattice points

If increase thermal activation is available (i.e. if the temperature is raised) further decrease in the free energy of the material can be brought about by the formation of new strain free grains. This process is termed recrystallization. These grains initially form in regions where the local degree of deformation is highest. Such sites include grain boundaries, sub-boundaries, deformation bands, twin intersections, and free surfaces. If inclusions or precipitates are present, they may also act as preferential sites for the nucleation of new grains. These new grains grow at the expense of the deformed structure until the whole matrix has been consumed. The process occurs either by migration of original grain boundaries or by sub grain growth. The recrystallized matrix has much lower dislocation density than the deformed material. The driving force for boundary migration is the decrease in free energy resulting from the decrease in density of imperfections. Above a minimum critical strain the rate of formation of recrystallization nuclei increases sharply with increasing strain.

The lowest temperature at which stress free grain appear in the structure of a previously plastically deformed metal is termed the recrystallization temperature. This depends upon the grain size, the severity of plastic deformation, and the presence of solute atoms or second phase particles.

If the recrystallized martial is further annealed at the same temperature, or at a higher temperature, grain growth usually occurs. Boundaries between annealed grains migrate and larger grains grow by consuming smaller ones, which disappear. Grain growth depends upon the fact that the grain boundary energy of the material is reduced due to the decrease in grain boundary area for a given volume of the material. In the absence of the complicating factors, e.g. second phase particles, this energy reduction leads to a relationship governing grain growth which can be expressed as

$D_t - D_0 = Kt^n$ ..... (1)

Where D_t is the average grain diameter after time t

D_0 is the initial grain diameter

K is a constant

The value of n is experimentally observed to be $\leq ½$

The presence of precipitates or inclusions drastically reduces the grain growth. The particles have a pinning effect on the grain boundaries. During grain growth a curved grain boundary usually migrates towards its centre of curvature. This is in the opposite direction to that usually observed in recrystallization. When grain boundaries in a single phase meet at angles other than 120^0, the grain included by the more acute angle will be consumed, and all angles approach 120^0 during the grain growth. When grain shapes in actual specimens are studied metallographically it is often seen that the approach is not very close.

Since dislocation density increases on plastic deformation, dislocation - dislocation interactions occur more readily in deformed materials. The motion of dislocation, therefore, requires larger applied stress in specimens which have higher dislocation density. Thus cold work increases the hardness of a material. Since recovery and recrystallization involve a reduction in density of imperfections, these processes are generally accompanied by a decrease in hardness of the material. In polycrystalline material, the grain boundaries also offer resistance to the motion of dislocation. The size of the grains can thus markedly affect the mechanical properties and grain growth softens the material. Hall and Petch have found that

$$\sigma_y = \sigma_t + Kd^{-1/2} \quad \text{(2)}$$

Where

σ_y Is the lower yield stress

σ_t and K are constants, characteristics of the martial, and

D is the average grain diameter.

The effect of annealing a plastically deformed metal on its grain size, internal stress, and strength is shown in fig. 2.

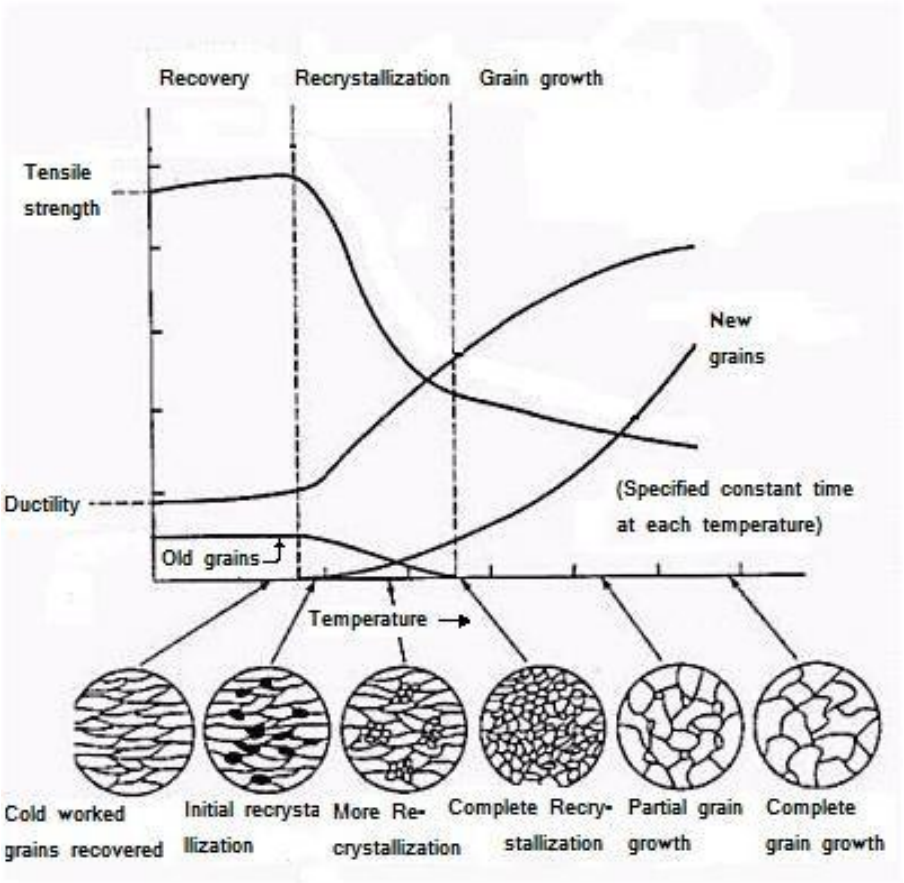

Fig. 2: Effect of annealing on tensile strength, ductility and grain

Preparation

You are given six samples prepared using the following steps:

1. Annealing of pure copper strip at 800°C for 1h and cooling in air after taking out of the furnace.
2. Subjected to deformation by cold rolling in steps by reducing the gap in a mill till the thickness reduces to half (~50% deformation).
3. Cutting into small pieces and heat treated at 400 - 800°C for different time periods.
4. Cold mounting, grinding and polishing of samples for microscopic examination.

Samples for microscopic observation

Sample number	Treatment	Sample number	Treatment
1	Annealed at 800°C for 1 h	4	Annealed at 400°C for 1
2	Annealed at 400°C for 10	5	Annealed at 400°C for 2
3	Annealed at 400°C for 30	6	50% deformed

Observation and task

1. Examine the microstructure of given samples using 100X magnification of the microscope and observe the effect of cold working and different heat treatments.

2. Measure the Rockwell hardness of three samples subjected to the following treatment

Treatment
50 % deformed
400°C for 2 hr.
800°C for 1 hr.

3. Draw schematic diagrams of the observations and discuss the effect of annealing temperature on hardness

4. Determine the ASTM grain size index number and actual grain sizes from the given photomicrographs of samples shown in the separate sheets attached. Plot the ASTM index number and grain size as a function of temperature for each treatment time period (i.e. 30 min. and 01 h). Use Jeffrie's planimetric ASTM method to measure grain size index number. The basic steps are as follows:

1. Inscribe a circle (or other shape) of known area A, on an image of magnification M.
2. Count the number (x) of grains those are completely within the area.
3. Count the number (y) of grains those are partially within the area.
4. Add x and y/2.
5. Divide the result from 4) by A and convert the result into grains per square inch at 100X. To convert the result into 100X equivalent multiply it by $(M/100)^2$.
6. Use the following ASTM relationship to measure the grain size:

$$\mathbf{n_a = 2^{(N-1)}}$$

Where n = number of grains per square inch and

N = ASTM grain size index number

Questions:

1. Explain the terms recovery, recrystallization and grain growth.
2. Does recovery influence the nucleation process of new strain-free grains?
3. State the factors responsible for raising the recrystallization temperature of a metal or alloy?
4. Will grain size continue to increase until the material is a single crystal?

9. Kerr effect

Object

Study of birefringence in a PLZT element (Kerr cell) and determination of Kerr constant by plotting the square of the voltage applied to the Kerr cell versus phase shift between ordinary and extraordinary beam.

Introduction

A light wave is an electromagnetic wave which is a transverse wave. It has both an electric and a magnetic component coupled perpendicularly. Sunlight and almost every other form of natural and artificial illumination like lamp or candle is referred as unpolaized light which vibrates in more than one plane. Such light waves are created by electric charge which vibrates in a variety of directions creating an electromagnetic wave which vibrates in a variety of directions. If the electric field vectors are restricted to a single plane by filtration of the beam with specific materials, then the light is referred to as **plane** or **linearly polarized** light as shown in figure1. This linearly polarized light which makes linear wave-front is the vector sum of two in phase electric components perpendicular to each other. When a quarter wave-plate is fixed into the back of a linear polarizer then these components becomes out of phase by 90° and the light obtained is referred as circularly polarized light which have a circular wave-front. Elliptically polarized wave is generated if the components are made out of phase by other than 0°, 90° or 180°.

In Fig.1 the polarizing direction of the first polarizer is oriented vertically to the incident beam so it will pass only the waves having vertical electric field vectors. The wave passing through the first polarizer is subsequently blocked by the second polarizer, because this polarizer is oriented horizontally with respect to the electric field vector in the light wave. The concept of using two polarizer's oriented at right angles with respect to each other is commonly termed as cross polarization.

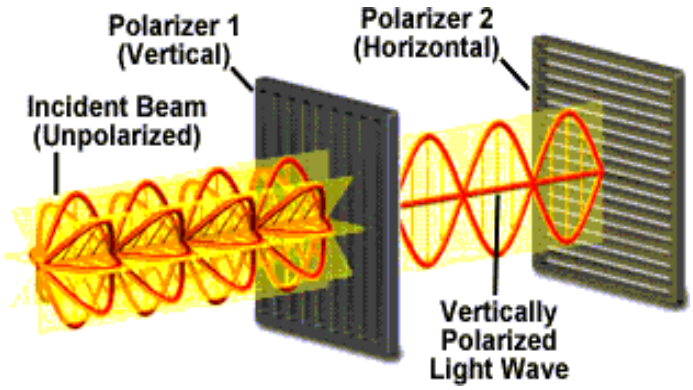

Figure1: Polarization of light waves

Linear polarizer’s can be divided into two general categories i.e. absorptive polarizer's where the unwanted polarization states are absorbed by the device and beam-splitting polarizer’s where un-polarized beam is split into two beams with opposite polarization states. Fresnel reflection polarizer’s, birefringent polarizer’s, thin film polarizer’s and wire-grid polarizer’s comes under beam splitting polarizer’s.

Wire-grid polarizer (WGP) is the simplest linear polarizer’s where the only wave which have its electric field component perpendicular to the wires passes through it while the component aligned parallel to the wires are mostly reflected back with a little absorption (Joule heating) because polarizer induces the movement of electrons along the length of the wires behaving same as a reflecting metal surface. It is shown in figure 2.

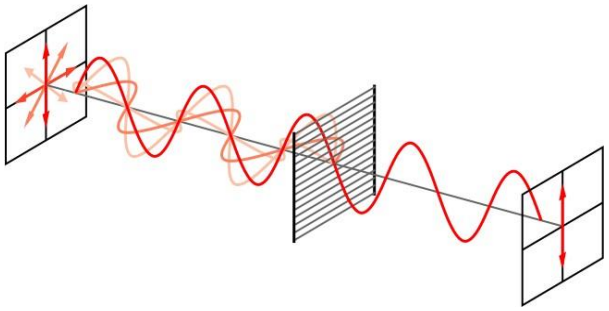

Figure2: Only the vertical components of the electric field are transmitted while the horizontal components are absorbed and reflected (not shown).

Some linear polarizer’s exploit the birefringent properties of crystals like quartz and calcite. **Birefringence** or double refraction is the property of some crystalline materials where the anisotropy is exhibited as a change of refractive index between light rays vibrating in different planes. When a beam of non-polarized light passes into a crystal of calcite the vibrational plane determines its velocity. Since refraction is a function of velocity, a beam of light is decomposed into two beams that refract at different angles. One plane of vibration realizes a higher refractive index and refract according to Snell's law. This is called the o**rdinary ray**. Another beam which vibrates at right angles to the O-Ray, realize a lower refractive index and bend at a lower angle. This beam is called the e**xtraordinary ray**, or E-Ray. Thus, two spatially separated rays exit through the birefringent object. These rays are linearly or plane polarized, and vibrates orthogonal to each other.

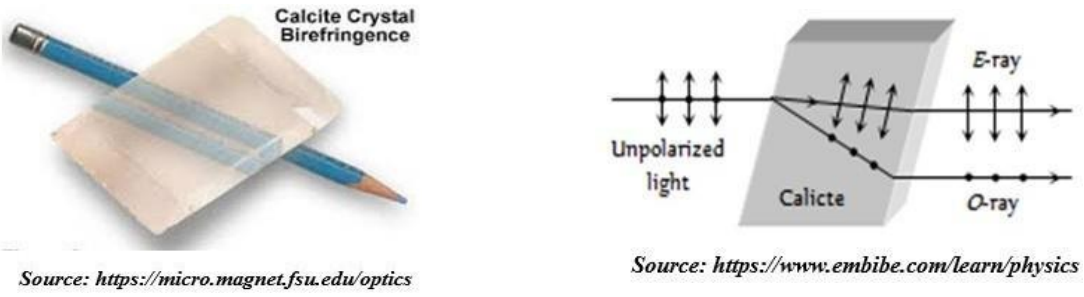

Figure 3: Double refraction through calcite crystal

Asymmetric crystals can be utilized to produce polarized light when an electric field is applied to the surface and that's what we do in Kerr cell and Pockel cell where the phase shift between these O rays and E rays (birefringence or double refraction) is carried out artificially as a function of electric field applied on it. In a Pockel cell the birefringence is proportional to the applied electric field (linear electro-optic effect) while in case of a Kerr cell it is proportional to the square of the E field. A typical Kerr cell (Nitro benzene in glass container) may require voltages as high as 30 kV while a Pockel cell can be operated at much lower voltage.

There are two cases of quadratic electro-optic effect or Kerr effect namely Kerr electro-optic effect where dc varying field is applied and optical Kerr effect where light source itself act as an a.c. source. When a Kerr cell is placed between two crossed linear polarizer's, no light is transmitted when the electric field is turned off, while nearly all of the light is transmitted for some optimum value of the electric field. Higher Kerr constant indicates the need of smaller electric field for complete transmission. Applications are high speed shutter, seven segments LCD etc.

Principal and task

Monochromatic, vertically polarized light impinges on a PLZT element (lead-lanthanum-zirconium-titanium compound) which is set in its holder at 45 ° to the vertical. An electric field is applied to the PLZT element and causes it to become bi-refractive. The phase-shift between the normal and the extraordinary light beam behind the PLZT element is recorded as a function of the applied voltage and it is shown that the phase-shift is proportional to the square of the electric field strength respectively of the voltage applied. From the constant of proportionality the Kerr constant is calculated for the PLZT element. The Kerr effect has usually been demonstrated with nitrobenzene in the past. Since nitrobenzene is very toxic and needs high voltages of some kV the PLZT element which only needs some hundred volts represents an attractive alternative. This one is transparent for wavelengths from 0.4 to 5.6 µm. Within the PLZT element there are already pre-polarized domains

which grow or which are reoriented by the applied electric field. In this way, the element becomes optically anisotropic and hence bi-refractive.

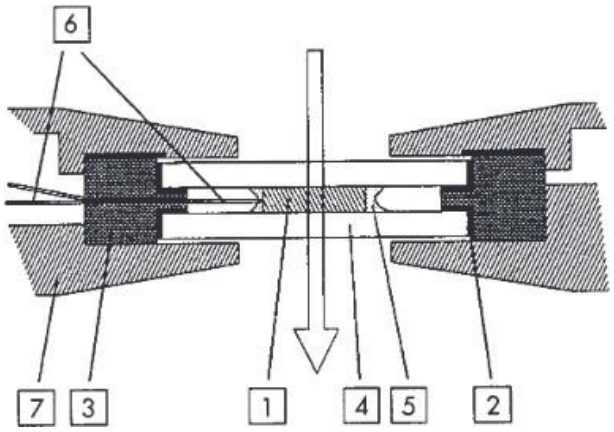

Figure 4: Cross section of the PLZT element. Element 1 is a parallelpiped of height = 8 mm, length = 1.5 mm and width = 1.4 mm

The width represents the distance between the electrodes. The electric field strength is given by the ratio of voltage applied over the distance between the electrodes. The path of the light beam within the element is equal to the length of the element. Active element (1) is encapsulated using silicon hermetics (2) an isolating ring (3) and glued between two glass plates (4). As optical glue (5) Canadian balsam was used. Wire (6) are fixed on the electrode faces of the element and connected with BNC socket on frame (7).

Equipment

Kerr cell, PLZT-element, high voltage supply unit, 0-10 kV, laser, He-Ne 1.0 mw, 220 V AC, polarizing filter, 02 in no's, optical bench, photo-element, universal measuring amplifier, digital multi meter 02 in no's, screened cable BNC, adapter BNC-socket/4 mm plug pair, connecting cord.

Set-up and procedure

The experiment for the demonstration of the Kerr effect is set up as shown in Fig. 5. The PLZT element is connected directly to the HV power supply whose voltage can be altered between 0 and 1000 Volt. The light source is a He/Ne laser.

Do not exceed 1000 V because it will damage the PLZT element.

As can be seen from Fig. 5, the light from the He/Ne laser, which is vertically polarized on passing through the polarizer, impinges on the PLZT element which is set in its holder at 45 ° to the vertical. The incident linearly polarized wave can be

regarded as the superimposition of two “in phase” oscillating waves which are polarized, one perpendicularly and the other parallel to the PLZT element and to the electric field that is applied to the PLZT element. The two light waves pass through the PLZT element at different speeds. The light wave which oscillates parallel to the electric field of the PLZT element is delayed relative to the light wave which oscillates perpendicularly to the applied electric field of the PLZT element. This produces a phase difference between the two waves and the light which has passed through the Kerr cell (PLZT element) will be elliptically polarized. This results in the analyzer, which is located behind the Kerr cell at 90 ° to the polarizer (cross polarization), no longer being able to extinguish the polarized light. For a phase difference between the two waves of $\lambda/2$ a linear polarized wave results from the superimposition of the two waves after they have passed through the PLZT element. This linearly polarized wave is turned by 90° with respect to the direction of incidence, e. g. with respect to the vertical. The applied voltage is therefore called the “half-wave voltage”. In this case the light intensity behind the analyzer which is sat in the cross condition will show a maximum. A silicon photodiode with amplifier is used as the detector for the luminous intensity behind the analyzer.

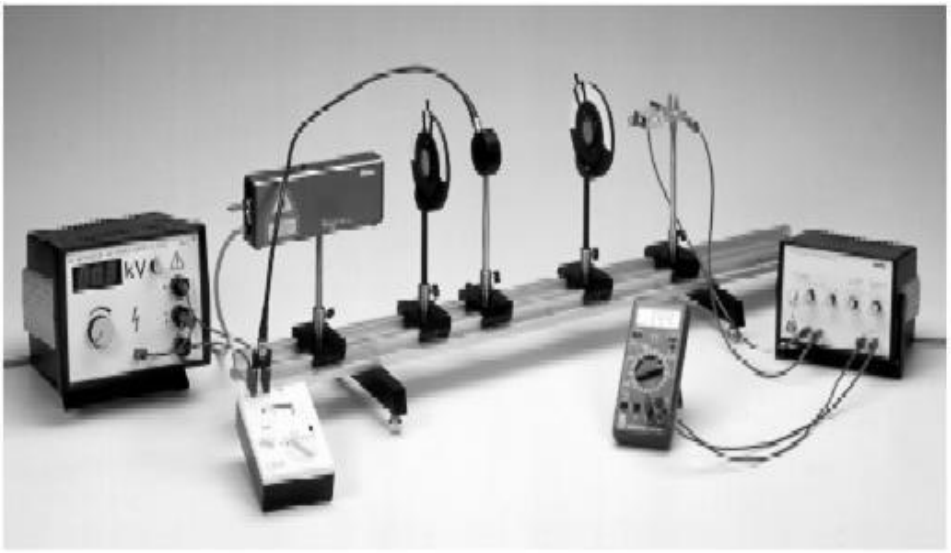

Fig. 5: Experimental setup for demonstrating the Kerr effect

Theory and evaluation

The light wave, whose field vector oscillates parallel to the electric field, is called the extraordinary beam whereas the wave oscillating perpendicular to the field is known as the ordinary beam. If the corresponding refractive indices are designated by $\mathbf{n_{ao}}$ and $\mathbf{n_a}$ and ℓ is the length in the PLZT element covered by the light, then the difference in optical paths for the two waves is given as

$$\ell(\mathbf{n_{ao}} - \mathbf{n_o})$$

This corresponds to a phase displacement of

$$\mathbf{D = 2\pi \ell/\lambda\ (n_{ao} - n_o)} \text{.....(1)}$$

where λ is the wavelength of the light in vacuum. (here λ = 633 nm).It can also be shown that the phase displacement is proportional to length l and the square of polarization P. If we anticipate that the polarization is a linear function of the electric field strength E and the proportionality factor is designated by $2\pi K$, then the following relation is obtained:

$$\mathbf{D = 2\ \pi\ k\ \ell E^2} \text{.....(2)}$$

K is the Kerr constant.

E can be expressed by the applied voltage V and the inter electrode distance d

$$\mathbf{E = V/d} \text{ .....(3)}$$

The luminous intensity I behind the analyzer is obtained for the given experimental apparatus (polarizer and analyzer crossed and at 45° to the electric field on the PLZT element) from the relationship (1):

$$\mathbf{I = I_o\ \sin^2 D/2} \text{.....(4)}$$

I_o is the luminous behind the analyzer when the polarizer and the analyzer are aligned in the same direction (not crossed) and the electric field on the PLZT element is zero. After substituting (2) in (4) and using (3), the followings is obtained:

$$\mathbf{I = I_o\ \sin^2\ \pi\ k\ \ell V^2/d^2} \text{.....(5)}$$

Solving the equation for V^2 gives:

$$\mathbf{V^2 = (d^2/\ \pi\ k\ \ell)\ arc\ sin\ \sqrt{(\ I\ /\ I_o)}} \text{ .....(6)}$$

where **π** is given in Radian.

By plotting V^2 against 2.arc sin $\sqrt{(I / I_o)}$ an approximately straight line is obtained and the Kerr constant can be derived from its slope, using eqn.6 because the geometrical dimensions l and d for the Kerr cell (PLZT element) are known. At a particular voltage the luminous intensity reaches a maximum (maxima) for the first time. In this case the normal and extraordinary beam are phase-shifted by 180°. Therefore this is called "half wave voltage" and is a function of the PLZT element composition and of the temperature. Also the number of detectable maxima may vary for different elements.

Problems

1. The phase-shift between the normal and the extra-ordinary light beam is to be recorded for different voltages applied to the PLZT-element respectively for different electric field strengths. The half-wave voltage V is to be determined.

2. By plotting the square of the applied voltage versus the phase shift between normal and extraordinary beam it is to be shown that the relation between the two quantities is approximately linear. From the slope of the straight line the Kerr constant is to be calculated.

Precautions

Never look directly into a non-attenuated laser beam.

1. Do not exceed 1000 V, this will damage the PLZT element.

2. He/Ne laser has to be switched on for about one hour to reach its equilibrium in power emission.

3. After each appreciable variation of the voltage applied to the PLZT element about five minutes have to elapse before the crystal structure has readapted and a representative luminous intensity reading can be taken.

4. All measurements have to be performed in a darkened room. The unpolarized portion of the light (background radiation) must also be taken into account.

Observation table:

V (volt)	**I**	**I / I_O**	**$D/2 = \text{arc sin } \sqrt{(I / I_O)}$**

10. Magneto-resistance and its field dependence

Objective

To study the magnetic field dependence of the transverse magneto-resistance of a given semiconductor sample

Introduction

The behaviour of the electrical resistance of a metal or a semiconductor in a magnetic field depends very much on its electronic structure. Magneto-resistance (change in electrical resistance on applying a magnetic field) is caused due to departure from the free electron model, when the magnetic field is applied at right angle to the electric current, a detailed theory (see references) shows that for small fields the transverse magneto-resistance

$$\frac{\Delta\rho}{\rho_o} = \frac{\rho-\rho_o}{\rho_o} \text{ a } B^2 \qquad \text{.... (1)}$$

Where ρ_o is the resistivity of the material in zero field, ρ is the resistivity in a magnetic field B. However, at higher fields the dependence is quite often linear. We have to study for low-field region however. Eq. (1) can also be written as

$$\frac{\Delta\rho}{\rho_o} = \frac{\Delta R}{R_o} = \frac{R-R_o}{R_o} \text{ a } B^2 \qquad \text{.... (2)}$$

Where R_0 is the resistance of the material measured between two points P and Q along the direction of the current I (x-axis) when no magnetic field is applied and R is the corresponding resistance when field B (along z-axis) is applied, as shown in Fig. 1.

If V_{PQ} is the potential difference between the points P and Q then the resistance $R = V_{PQ} / I$ where I is the current through the sample.

If the magnetic field is parallel to the current direction then the change of resistance is called the longitudinal magneto-resistance. Here also equation (1) holds good except that the constant of proportionality between $\Delta\rho / \rho_0$ and B^2 is much smaller than that obtained in transverse magneto-resistance. Here we are going to study only the transverse magneto-resistance.

Experimental Arrangement

A sample holder inbuilt with spring loaded four point probe is taken and sample is placed which is to be characterized (here n type Ge wafer). The sample current I is supplied from outer probes by a constant current source (0-20mA) and the voltage across them is measured through inner probes using a multi-meter keeping in voltmeter mode as shown in figure1. The magnetic field is increased by varying the power supply (here bi-polar) connected to the electromagnet coils.

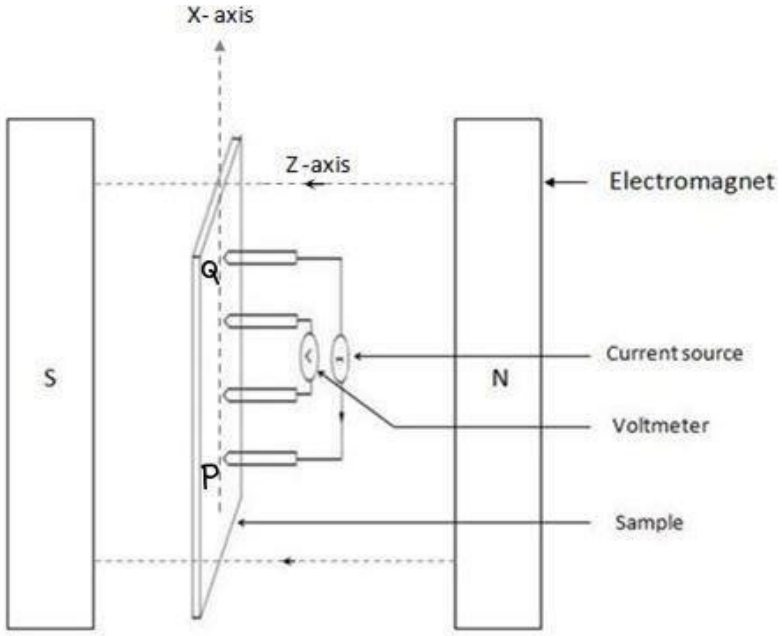

Figure 1: Schematic diagram for magneto-resistance setup

Place the magneto-resistance probe between the pole pieces of the electromagnet so that the field is perpendicular to the direction of the sample current. The magnet current is provided by a power supply (bipolar supply 0 to $\pm$30 amp.) and is measured by a built-in ammeter. The magnetic field can be obtained directly using a Gauss meter or from the calibration curve provided. Here the measurements are quite simple. For every value of the magnetic field the sample current has to be reversed (both +I and -I) and the voltage V_+ and V_- measured to minimize the effect of thermal voltage. Then V_{PQ}/I (with $V_{PQ} = (V_+ - V_-)/2$) gives R at the field B. Its value at B = 0 gives R_0. A graph should be drawn between $\Delta R/R_0$ and B(gauss) on a log-log scale, the slope of which should be compared with the theoretical slope of 2 as given in Eq. (2). The other alternative is to fit to $\Delta R/R_0 = CB^n$ and find n.

Precautions

(1) Do not exceed 5 mA sample current.

(2) Increase the power supply current slowly and carefully.

Questions

1. Is it necessary to reverse the magnetic field in this experiment? Discuss why do you reverse the sample current?
2. How will you orient your sample with respect to the direction of the magnetic field?
3. What are the applications of the phenomenon of magneto-resistance in science and technology?
4. Suggest a method of measuring voltages of the order of a few μV other than using a micro-voltmeter.
5. Will the magneto-resistance change if you heat your sample to say, 50^0C, above room temperature?

References

1. W.C. Dunlap, An Introduction to Semiconductors, John Wiley and Sons, Inc. (1957), pages 111-114, 178-190.

2. E.H. Putley, The Hall Effect and Related Phenomena, Butterworths, London (1960), pages 23-26, 166-175.

3. G.L. Pearson and H. Suhl, Phys. Rev., **83**, 768 (1951).

11. Tensile and hardness tests

Object

Investigate the behavior of specimens of two different materials under tensile test and to find out the Rockwell hardness number for the same materials using proper Rockwell scale. The materials to be tested are aluminum and steel.

Theory

The tensile test is the basic test carried out to determine the mechanical properties of materials such as metals, polymers composites, fibers etc. Properties such as Young's modulus, Yield strength, Ultimate Tensile Strength and ductility can be determined. In this test the ends of a test piece are fixed into grips connected to a straining device and to a load measuring device. If the applied load is small enough, the deformation of any solid body is entirely elastic. An elastically deformed solid will return to its original form as soon as load is removed. However, if the load is too large, the material can be deformed permanently. The initial part of the tension curve which is recoverable immediately after unloading is termed elastic part and the rest of the curve which represents the manner in which solid undergoes plastic deformation is termed plastic part.

When elastic deformation occurs in metallic and ceramic materials, the interatomic bonds are stretched or compressed and the strain is nearly proportional to the stress. Because load and deformations are not the properties of the materials, the characteristic plot is drawn between stress and strain. The slope of the elastic region is known as modulus of elasticity and is a characteristic of the material. Greater force of attraction between atoms results into the higher modulus of elasticity.

The stress below which the deformation is essentially elastic is known as the yield strength of material. In some material the onset of plastic deformation is denoted by a sudden drop in load indicating both an upper and a lower yield point. In such cases it is easy to specify the yield point as a measure of strength of the material. However, some materials do not exhibit a sharp yield point. The factors that give rise to the yield are small initial number of mobile dislocation, a rapid dislocation multiplication under strain and strong stress sensitivity of dislocation velocity. At start the small number of mobile dislocation cannot move sufficiently fast to produce required strain rate and hence stress increases to produce that rate. With rise in stress the number of mobile dislocations increases and also they move faster until the strain rate of the crystal equals the applied strain rate and stress stops rising. Continuous multiplication of dislocation creates more than enough dislocations. It increases the dislocation density and the stress increases again. This happens beyond elastic limit. The material in this stage is called strain harden. The increase in external stress is due to interaction of moving dislocation and existing dislocations.

Plastic deformation occurs by slipping of adjacent molecules with respect to one another because intermolecular attractive forces are weaker than intramolecular

forces. At small extensions in plastic region, strain hardening dominates and the load increases. However, at larger extensions the cross-section of the specimen decreases to such an extent that strain hardening cannot compensate for the decrease in cross-section and thus the load passes through a maximum and then begins to decrease. At this stage the "engineering stress" which is defined as the ratio of the load on the specimen to original cross-sectional area, reaches a maximum value. Sometimes it is called ultimate tensile strength (UTS). Further loading will eventually cause 'neck' formation and rupture. Strain hardening continues up to the point of rupture but ordinary stress –strain curves for ductile materials do not exhibit this beyond UTS due to reduction in cross-section. The true stress can be found out by dividing the load by the actual true area of cross section at the moment.

$$\sigma_{true} = \frac{\text{Load}}{\text{True Area}}$$

Also $\sigma_{engg} = \frac{\text{Load}}{A_0}$; where σ_{true} and σ_{engg} are known as true and engineering stresses.

From above we have $\sigma_{true} = \sigma_{eng.} \frac{A_0}{A_t}$

If A_0 = initial cross section, or at time t=0
L_0 = length of the specimen at t=0
A_t = true cross section at time t
L_f = length at time t

Then assuming volume of the specimen being constant during test, $A_0 L_0 = A_t L_f$

Thus $\sigma_{true} = \sigma_{eng.} \frac{L_F}{L_0} = \sigma_{eng.} \frac{dL + L_0}{L_0} = \sigma_{eng.} (1 + e_{eng.})$

Or $\mathbf{\sigma_{true} = \sigma_{eng.} (1 + e_{eng.})}$

Where e_{eng} is engg. strain.

Similarly true strain is defined as the incremental change in length per unit length. The total true strain is

$e_{true} = \int de = \int_{L_0}^{L_f} \frac{dl}{l}$ or $e_{true} = \ln \frac{L_f}{L_0} = \ln \frac{A0}{A_t}$

Hence $\mathbf{e_{true} = \ln (1 + e_{engg.})}$

Thus a true stress vs strain curve can be plotted from tensile data and it shows that the metal gets stronger up to the point of rupture. Nucleation of crack takes place when plastic flow of material occurs in local regions (neck). High stress concentrations occur on the boundaries of such regions and cracking occurs when the stress concentration equals the cohesive strength of the material.

Generally tension test is done at room temperature and the tensile load is applied slowly. Round or flat specimen can be used for tension testing. The end of the specimen could be smooth, shouldered or threaded. The load on the specimen can be applied mechanically or hydraulically depending on the machine type.

Main Components of the Universal Testing Machine are as follows –

1. Load frame-The two strong side supports on the machine.

2. Load cell- It consists of a force transducer which when sense a force, deform a strain gauge. Strain gauge measures the deformation as a change in electrical resistance.

3. Cross head- A movable part, controlled to move up and down. Some machines can program the crosshead speed or conduct cyclical testing, testing at constant force, testing at constant deformation, etc.

4. Extensometer- Sometimes used for measuring extension or deformation accurately.

5. Output Device- Some older machines have chart recorders for result. Now a day's computer interface is frequently used for analysis and printing purposes.

6. Test fixtures – These are different type of grips, specimen holding jaws and three point test fixture etc.

Procedure

Using the permanent marker and venire calliper mark the two ends of gauge length on the straight portion of the specimen. The marked length should be symmetric about the centre of specimen. Mark lines after every 5 mm. Measure width and breadth of reduced cross section with vernier callipers at 5 different points. Calculate the average values of both width and breadth. Draw a neat drawing of the specimen with tolerances.

Mount the sample on machine using suitable grips. Make sure that the grip is tight. The sample should be mounted parallel to axis of the testing machine.

Turn on the computer which is connected to the tensile testing machine. Open testing software and set the following parameters

1) Cross sectional area and related dimensions.
2) Gauge length (60 mm)
3) Speed (2mm/min)
4) Preload (20 kgf)

Start the test. Once the component is fractured the test will automatically stop. Save the data.

Task

Perform following tasks for both aluminium and steel specimens

1) Draw neat figure of specimen.
2) % Elongation
    a. From initial and final gauge length
    b. From recorded data
3) Change in cross sectional area at marked intervals and at the necking region.
4) Plot following graphs
    a. Load vs deflection curve
    b. Engineering stress – strain curve
    c. True stress – strain curve
5) Obtain following material properties
    a. Yield strength
    b. Ultimate tensile strength
    c. Young's modulus
    d. Ductility
    e. Toughness
    f. Upper and lower yield point

Questions

1) Compare given sample with ASTM standard.
2) Compare properties found from experiment with standard values.
3) Why % elongation values measured from two different techniques mentioned in task 2 are not equal? What is % difference between two values? Which method is preferred?

4) Why stress strain-curve of steel shows phenomenon of upper and lower yield point? Why same phenomenon is absent in stress-strain curve of Al?
5) Compare the ductility of Aluminium and Steel. Comment on the result obtained.
6) Why materials with fcc lattice is more ductile than materials with bcc lattice?
7) One can observe small step at the starting of the load vs deflection graph when test is conducted in Kalpak UTM. Find the reason for occurrence of that step.

Rockwell hardness test

The most widely used hardness test is the Rockwell hardness test. Its general acceptance is due to its speed, freedom from personal error, ability to distinguish small hardness differences in hardened steel, and the small size of the indentation, so that finished heat-treated parts can be tested without damage. This test utilizes the depth of indentation, under constant load, as a measure of hardness. A minor load of 10 kg is first applied to seat the specimen. This minimizes the amount of surface preparation needed and reduces the tendency for ridging or sinking in by the indenter. The major load is then applied, and the depth of indentation is automatically recorded on a dial gage in terms of arbitrary hardness numbers. The dial contains 100 divisions, each division representing a penetration of 0.002 mm. The dial is reversed so that a high hardness which corresponds to a small penetration, results in a high hardness numbers. This is in agreement with the other hardness numbers but unlike the Brinell and Vickers hardness designations, which have units of kilo grams per square millimeter (kgf mm^{-2}), the Rockwell hardness numbers are purely arbitrary.
One combination of load and indenter will not produce satisfactory results for materials with a wide range of hardness. A 120^{o} diamond cone with a slightly rounded point, called a Brale indenter, and 1.6 and 3.2 mm-diameter steel balls, are generally used as indenters. Major loads of 60, 100, and 150 kg are used. Since the Rockwell hardness is dependent on the load and indenter, it is necessary to specify the combination which is used. This is done by prefixing the hardness number with a letter indicating the particular combination of load and indenter for the hardness scale employed. A Rockwell hardness number without the letter prefix is meaningless. Hardened steel is tested on the C scale with the diamond indenter and a 150-kg major load. The useful range for this scale is from about HRC 20 to HRC 70. Softer materials are usually tested on the B scale with a 1.6 mm-diameter steel ball and a 100-kg major load. The range of this scale is from HRB 0 to HRB 100. The A scale (diamond penetrator, 60-kg major load) provides the most extended Rockwell hardness scale, which is usable for materials from annealed brass to cemented carbides. Many other scales are available for special purposes. The Rockwell hardness test is a very useful and reproducible one provided that a number of simple precautions are observed. Most of the points listed below apply equally well to the other hardness tests:

1. The indenter and anvil should be clean and well seated.
2. The surface to be tested should be clean and dry, smooth, and free from oxide. A rough-ground surface is usually adequate for the Rockwell test.
3. The surface should be flat and perpendicular to the indenter.
4. Tests on cylindrical surfaces will give low readings, the error depending on the curvature, load, indenter, and hardness of the material. Theoretical and empirical corrections for this effect have been published.

5. The thickness of the specimen should be such that a mark or bulge is not produced on the reverse side of the piece. It is recommended that the thickness be at least 10 times the depth of the indentation. Tests should be made on only a single thickness of material.

6. The spacing between indentations should be three to five times the diameter the indentation.

7. The speed of application of the load should be standardized. This is done by adjusting the dashpot on the Rockwell tester. Variations in hardness can be appreciable in very soft materials unless the rate of load application is carefully controlled. For such materials the operating handle of the Rockwell tester should be brought back soon as the major load has been fully applied.

Test Procedure

1. Select and insert indenter as per the test purpose.
*Measuring point should be at least 4d away from the centre of any pre existing indentation and at least 2d away from the edges of the specimen.
Where d = Diameter of the Indentation.

2. Place the specimen on table/anvil and select the load required as per scale.
*The specimen should be cleaned. Remove oil/dust etc.

3. Bring the specimen close to the indenter with the help of vertical shift handle. The long needle position on the dial gauge should be around **C30** (**B60**). When the specimen touches the indenter, both long and short needles start to move.
*The indenter is most frequently damaged by hitting-up when removing the anvil or placing and removing the specimen. Care must be taken.

4. Elevate the specimen till the short needle moves to a red mark on the dial gauge and the long needle points upward. “This is the position when the initial load of 10 Kg is applied to the specimen.”

5. Turn the dial with the dial gauge adjusting lever and set the long needle to **C 0 (B30)**.

*Gauge lever can be adjusted within ±5 graduations, hence long needle should be set in the range otherwise change the measuring position.

6. Set the load holding timer (15 second is recommended) and apply the test load by pressing the switch given.

7. Testing procedure is now automatically performed and it is completed in the following steps:
   (a) Loading (Load is applied to the specimen).
   (b) Load holding (The applied load remains constant for a time being as per the setting of timer).
   (c) Load releasing (Load is removed automatically).
   (d) Now the long needle indicates the Rockwell hardness of the specimen.

   *Dial figures – Read the Black scale for Diamond indenter.
   – Read the red scale for Steel ball indenter.

8. Turn the shaft handle in reverse direction and lower the specimen.

9. If the surface to be tested is cylindrical the measured value of hardness will be lower than the true value. It should be corrected with the help of an standard correcting table.

10. The test load must be gradually increased without shock. Load application speed control knob should be set from 40 to 60.
    *If it is set at 30 or less the test load cannot be applied.

11. The accuracy of the tester can be checked by using standard hardness pieces.

12. Energy band gap by optical absorption

Objective

To determine the energy gap of a semiconductor / insulator by optical absorption method

Principle

Consider the energy band diagram of an intrinsic semiconductor or insulator (fig 1). Here $E_g = E_c - E_v$ represents the energy of the band gap or forbidden gap. For excitation of any electron from valence band to conduction band, energy equal to or larger than E_g is required. Similarly for extrinsic semiconductor (where energy levels exists near conduction band and valence band) energy corresponding to band gap (E_g) or larger than E_g will be required for band to band transition. The principle of determining this band to band excitation essentially involves detection and measurement of wavelength/ energy of optical radiation / photon that gets absorbed by a given semiconductor/insulator.

In this experiment, suitable radiation is allowed to fall on a thin film of a semiconductor and the percentage transmission and reflection are recorded as a function of wavelength.
While the photons of energy less than the band gap (E_g) are transmitted, others having energies equal to or more than E_g are absorbed. If the energy of photon (precisely wavelength of incident optical radiation) is varied continuously, the transition point at which radiation is absorbed can be accurately determined from the data obtained from transmission or reflection spectrum.

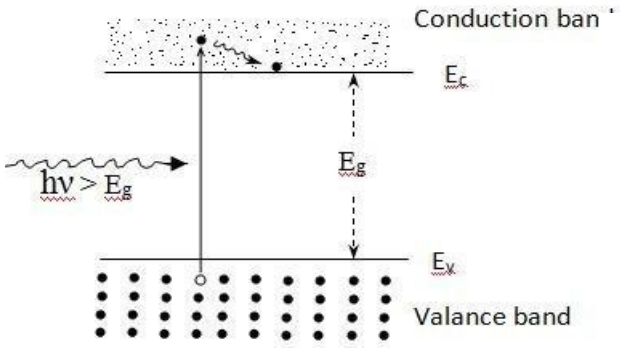

Figure - 1

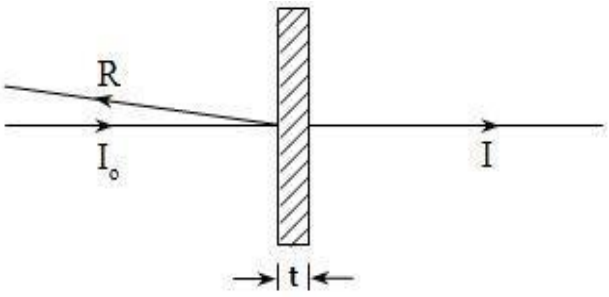

Figure – 2

I*, *R* and *I*$_o$** *are the incident, reflected and transmitted beam. Sample thickness is* ***t

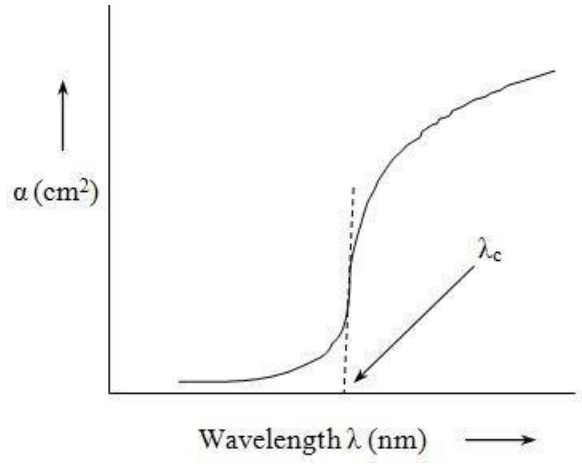

Figure - 3

Procedure

A nickel film is deposited on a clean substrate and then oxidized to form nickel oxide (NiO) for transmission and reflection measurements by a spectrophotometer.

1. Substrate Cleaning:

The substrate chosen is a quartz/glass plate 20 mm x 20mm x 1mm. For cleaning, follow steps below.

a. Clean the quartz/glass plate with soap solution/detergent and wash in distilled water. Let it dry.
b. Use trichloroethylene to clean the quartz plate in ultrasonic cleaner for about 5 minutes.
c. Repeat step (b) using acetone and methanol in succession.
d. Let the clean quartz plate dry in a dust free environment.

2. Film Deposition

a. Clean the nickel piece of known weight (22 mg for film thickness of 400Å) in trichloroethylene, acetone and methanol in succession in an ultrasonic cleaner and then let it dry. Now place nickel in the filament/boat, already mounted in working chamber of the vacuum coating unit.
b. Mount the cleaned substrate at a distance of 10 cm vertically above the filament/boat in the working chamber.
c. Place the bell jar back with proper greasing of the rubber gasket.
d. Follow the pumping system steps to create vacuum 10^{-5} torr or better.

e. Now pass the current through the filament/boat, use variac and turn it clockwise (watching the current meter and filament) until the nickel starts melting. Maintain the currents at slightly higher level so as to allow evaporation of the nickel piece completely. Now decrease the current through the filament slowly.
f. Wait for ten minutes for filament to cool down and close the baffle valve and then introduce the air in the work chamber. Remove the nickel coated quartz plate and store it in vacuum desiccators.
g. Place back the bell jar and pump it down before shutting down the coating unit.

3. Oxidation Process

a. Nickel film is now oxidized by heating in oxygen atmosphere/ air at 400^{o}C. For this insert the substrate containing the nickel film in a furnace already held at 400^{o}C.
b. Allow oxygen to flow at the rate of 75-100ml/min through the quartz tube.
c. After oxidation at 400^{o}C for 1 hour, slowly decrease the furnace power and allow it to cool down to room temperature while maintaining the oxygen flow.
d. Take out the quartz plate and store in dust free chamber.

4. Optical Measurement

A block diagram of Hitachi 150-20 UV-VIS spectrophotometer is given in fig 4. The light emitted from the sources passes through the stray light cut-filter F and slit S_1 and goes to the monochromater utilizing a concave diffraction grating G. The monochromatic light passes through exit slit S_2 and toroidal mirror M, where it is divided into two beams, one is used for reference and the other for the sample. These two light beams then enter the sample compartment consisting of 60 mm diameter sphere whose inside surface is coated with white paint (barium sulphate of high reflectivity). The sample beam strikes toroidal M first and is reflected at right angle to the initial direction. These two beams after passing through the transmissive samples are reflected repeatedly from the inside surface of the sphere, get finally concentrated at opening of the detector (PMT R928 of ultra-high sensitivity) placed at the base of the integrating sphere, and converted into electrical signal for display on monitor as % transmission verses wavelength plot. The entire spectrum can be manipulated using built in program and hard copy made with the printer provided. For reflectance measurement, the sample and reference are placed at the position R and R', respectively.

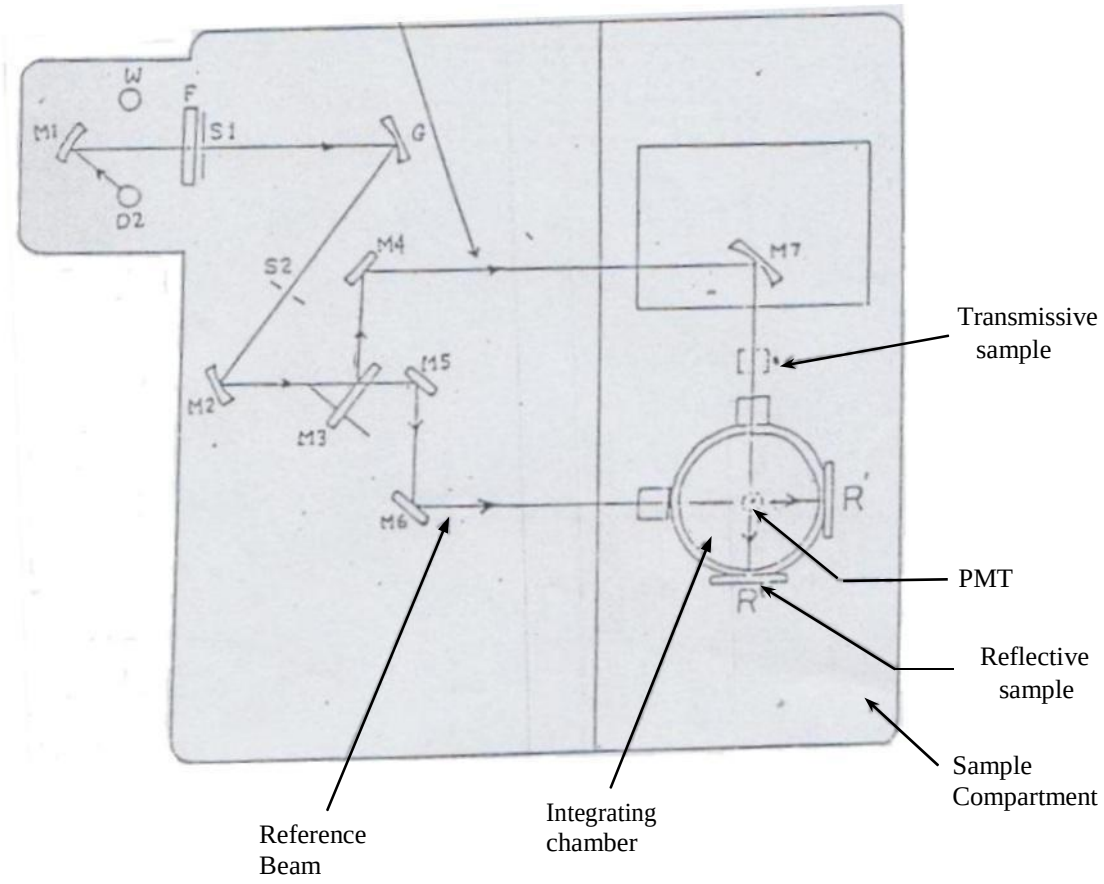

W: Tungsten lamp

D2: Deuterium discharge lamp

M1: Condensing mirror

F: Filter

S1: Entrance slit

G: Grating

S2: Exit slit

M2, M7: Toroidal mirrors

M3: Rotating mirror

M4,M5,M6: Plane mirror

PMT: Photomultiplier tube

Figure 4: Ray diagram of UV visible spectrophotometer

The loss of radiation on passing through thin film is attributed to absorption, reflection and scattering (fig 2). The ratio of transmitted intensity (I) to the incident intensity (I_0) when light passes through an absorbing media (say a thin film) is given by the Lamberts law

$$I = I_0 \exp(-\alpha t) \quad \text{.....(1)}$$

Where α is the absorption coefficient and t is the film thickness. The ratio I/I_0 is called transmittance (T). The expression is however applicable to the ideal situation when no reflection of the incident light occurs from the film surface. Consider the reflection coefficient R of the film front surface, the resultant transmittance (T) is given by

$$I/I_0 = T = (1- R) \exp(-\alpha t) \quad \text{.....(2)}$$

If 't' is known then the relation (2) can be used to obtain absorption coefficient α from the transmittance and reflectance measurements. The absorption coefficient (α) verses wavelength plot (fig 3) can then be made. This is used to find out wavelength λ_c where considerable absorption occurs. The value of E_g is thus obtained from the relation

$$E_g = h c/ \lambda_c \quad \text{..... (3)}$$

Where h is Planck's constant and c is the velocity of light

Alternatively,

The energy band gap of direct semiconductor (E_g) is related to the absorption coefficient (α), Such that

$$(\alpha h\nu)^2 = A\ (h\nu - E_g), \qquad h\nu > E_g$$

Where 'A' is a constant and depends on the material, h is the Plank's constant and ν is the frequency of the radiation. Thus, $(\alpha h\nu)^2$ verses hν plot corresponds to a straight line with Intersection at the abscissa giving E_g. However, absorption begins at some $E < E_g$ and increases exponentially up to E_g due to band tailing caused by defects present. For this reason, extrapolation of linear portion is undertaken in the $(\alpha h\nu)^2$ verses hν plot to determine E_g by the intersection on the abscissa.

Samples

A. NiO prepared by depositing nickel film of thickness 40 nm by e^- beam/ thermal evaporation (as described above) and then subjected to oxidation in air at 400°C for 1h.

B. ZnO films prepared by spin coating using homogeneous solution of zinc acetate dehydrate in ethanol with monoethanolamine (MEA) as stabilizer and final annealing at 500 °C for 1 h in air.

Tasks/questions

1. Run the UV-VIS spectrophotometer in the wavelength range 320-900 nm following instructions provided and obtain percentage transmission (%T) verses wavelength (λ) plots for sample 'A' and 'B' on the TV monitor screen with quartz/glass substrates reference. Note down the % T values in 1/0.1 nm step using cursor in the following intervals.

   (A) NiO 320 – 450 nm (B) ZnO 360 – 450 nm

2. Determine fractional change in film thickness by oxidation. Assume complete oxidation of nickel film of thickness 40 nm.

   Given: Atomic weight of Ni = 58.71, Atomic weight of Oxygen = 16
   Density of Ni = 8.9 g cm^{-3} and that of NiO = 6.67 g cm^{-3}

3. Obtain percentage reflectance (% R) data provided for NiO sample. Find out the absorption coefficient (α) using transmission and reflection data from eq. (2) with the value of NiO film thickness determined.

4. Draw $(\alpha h\nu)^2$ verses (hν) plot and deduce the value of energy band gap (E_g) by extrapolation of the linear portion.

5. Draw α verses λ plot (fig. 3). Determine E_g as described and compare with the result arrived at in step 4.

6. Draw $(\alpha h\nu)^2$ verses (hν) plot for ZnO sample with film thicess t = 120 nm. Determine (E_g) using percentage transmission (%T) and reflectance (% R) = 0.

7. Can you find (E_g) from transmission spectra alone? Justify your answer.

8. How will you ensure the occurrence of oxidation?

References

1. Optical processes in semiconductors, J. I. Pankove, Prentice Hall (1971)
2. Semiconductors, R. A. Smith, Acadmic Press (1964)
3. Solid State Semiconductor Devices, B. G. Streetman, Prentice Hall (2005)
4. Thin Film Phenomena, K. L. Chopra, Mc Graw Hill (1969)

13. X-ray powder diffraction pattern and its interpretation

Introduction

The crystalline material is reduced to a very fine powder and placed in a beam of monochromatic X-rays. Each particle of the powder is a tiny single crystal oriented randomly with respect to the incident beam. Among these tiny crystals, there will always be a certain fraction whose (hkl) planes make an angle θ, corresponding to Bragg's law of diffraction ($2d \sin\theta = \lambda$), with the incident beam and lie at the same time in all possible rotational positions about the axis of the incident beam. Thus each set of (hkl) planes give rise to a cone (fig. 1) with a semi-vertical angle (2 θ). The cone arising from differently spaced planes intersect the photographic film(cylindrical strip in a Debye Scherrer camera) in curves (except for $2\theta = 90^0$, when in line). When the strip is unrolled and laid out flat, the resulting pattern after processing the photographic film looks like the one illustrated in fig. 2. Each line/curve is made of small spots (each appearing from a tiny single crystal) lying so close together that they form a continuous curve/line. From the measured position of a given diffraction line (or ring) on the film, θ can be determined and knowing the wavelength λ of the incident X- rays, one can calculate the d-spacing of the crystal planes giving rise to diffraction.

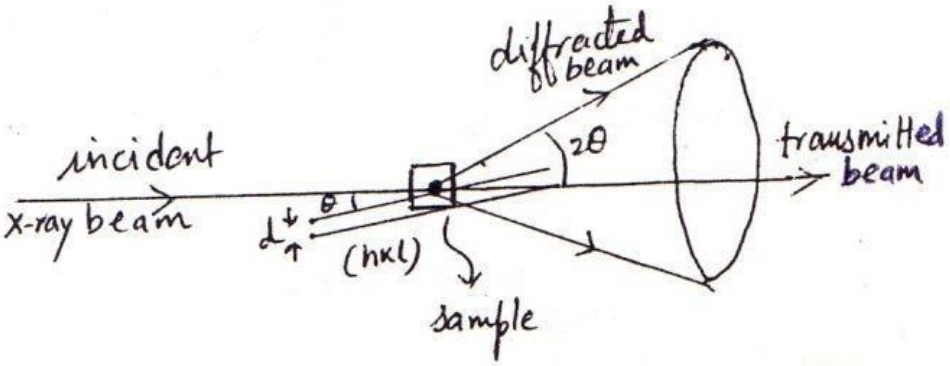

Figure - 1

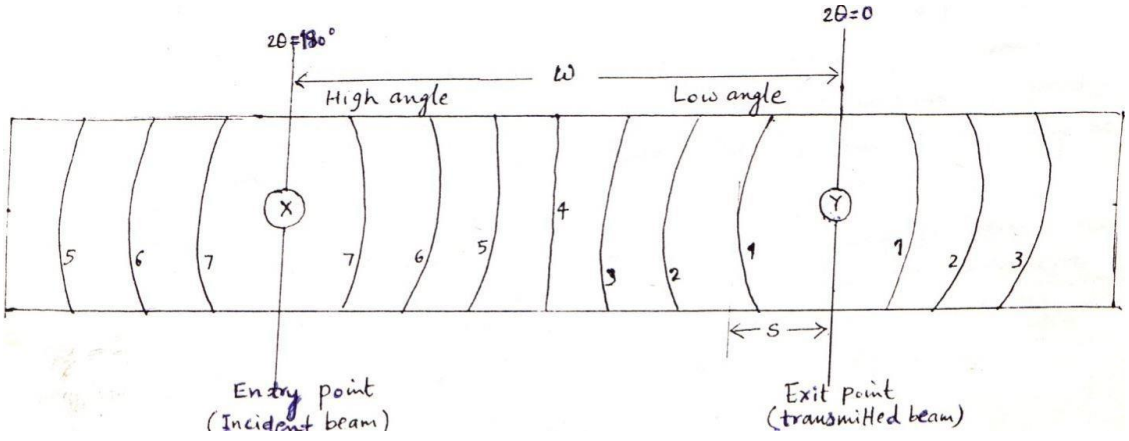

Figure - 2

Debye Scherrer camera

It consist of a cylindrical chamber with a light tight cover, a collimator to admit and define the incident beam, a beam stop to confine and stop the transmitted beam, a means of holding the photographic film tightly against the inside circumference of the camera, and a specimen holder that can be rotated. A camera of a particular diameter(say 57.3mm, is often found suitable for most work, keeping in view the geometrical considerations to facilitate calculations (fig.3).

$W = \pi R = \pi * 57.3/2$ mm = 90mm

Since W = 90mm corresponds to $2\theta = 180^0$ (or $\theta = 90^0$), each mm separation from the point where the transmitted beam strike the film (Y in fig. 2) will correspond to $\theta = 1^0$. In practice , at X and Y (fig. 2) holes are punched in the film for accommodating the collimator and beam stop, respectively.

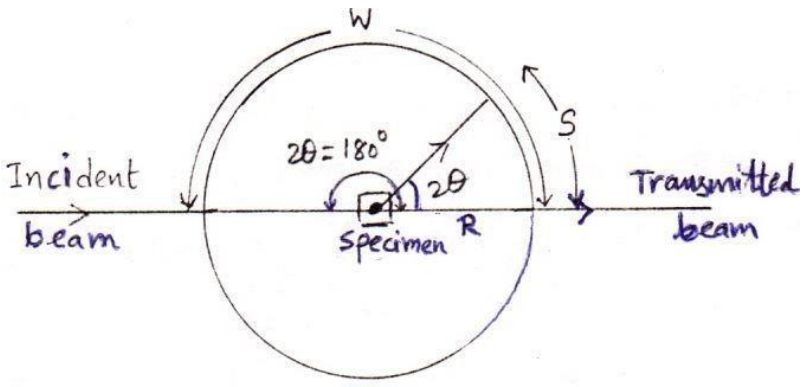

Figure - 3

Experimental

Specimen Preparation

Sample is converted into a fine powder by filing or by grinding in a small agate mortar and passed preferably through a 200/300 mesh screen. The fine powder thus obtained is then annealed in an evacuated glass or quartz capsules in order to relieve the strains induced during filing/grinding process. The final sample in the form of a thin rod of a diameter ~ 0.05mm or less and about 10mm long is prepared by coating the powder on the surface of a fine glass fibre with glue or petroleum jelly. Alternatively, powder is packed into a thin walled tube of a weak X-ray absorbing substance such as cellophane or lithium borate glass, or extruding a mixture of powder and binder through a small hole. Polycrystalline wire may be used directly.

The specimen rod is mounted in its holder using plasticine such that it lies accurately along the axis of the Debye Scherrer camera, when the holder is rotated (that means no wobbling is seen on rotation). An electric motor is used to rotate the sample during exposure.

Film loading

Two holes are punched in the photographic film (fig.2) so that it may be slipped over both the entrance collimator and the beam stop. These allow to determine the positions on the film where incident beam entered the camera and where the transmitted beam left it. The point (2 $\theta = 180^0$), where the incident beam entered the camera, is half way between the measured positions of curves/lines 7,7 ; similarly, the point Y(2 $\theta = 0^0$), corresponding to the exit of the transmitted beam is half way between lines 1,1. The difference between the positions X and Y gives w and θ is found by proportion :

$$2\theta/\pi = s/w$$

Note that the pairs 1,1; 2,2, etc….. belong to the cones emerging from the sample and intersecting a cylindrical strip. The photographic film always shrinks during processing and drying – amounting thereby to effective change in the camera radius . However, the above procedure of measuring XY separation provides correction for film shrinkage automatically.

Radiation

In our case Fe K_α radiation (λ = 1.937Å) or CrK_α (λ = 2.2910 Å) radiation with an appropriate filter.

Recording procedure

The Debye Scherrer camera loaded with the sample and the photographic film is mounted on a stand provided on the X-ray generator. The stand is then adjusted to desired height. Its platform is movable in the horizontal plane and can be lowered or lifted upwards from one end. By manipulating these controls, one makes sure that the –ray beam enters the collimator, passed through the sample and reaches the beam stop. A motor is then connected to the sample holder from outside for rotation of the sample. With this, the set-up becomes ready for exposure for any desired length of time (say 2 hours or more). Subsequently, the film is developed, fixed, washed and then hanged for drying.

Measurements

For measuring the line positions, the film is placed on an opal-glass plate of an illuminator equipped with a vernier and the cross-hair.

The slider is moved such that the cross-hair makes a tangent with the diffraction curve/ring/line and the position is then noted. Such readings are taken for all the diffraction lines by making the slider in one direction from one end of the photographic strip to another.

The amount of blackening caused by a particular line on the photographic film is a measure of the diffracted intensity. The following scheme can be used to mark each line for intensity measurement:

Very strong (v.s.), strong plus (s^+), strong (s), strong minus (s^-), weak (w), very weak (vw) etc. Alternatively one can assign a number 100 to the strongest line and then relatively grade each line by judgment. Needless to say that intensity can also be measured experimentally by a densitometer.

Interpretation

The positions of diffraction rings/lines on a powder photograph can be used to compute the corresponding Bragg angle θ's (as described in sections 3.2 and 3.5). Now, if the unit cell of the material is known, indexing of diffraction lines becomes straight forward. The d-values are calculated for all possible combinations of indices(hkl) for the system in question(or noted from the diffraction files) and compared with the derived d_{hkl} values from the measurements using the well known Bragg's law:

$2d_{hkl} \sin \theta_{hkl} = \lambda$

The indices can therefore be assigned to each diffraction line. Alternatively, one computes $\sin^2 \theta$ values for observed Bragg angles (θ's). Take for example, a cubic system of unit cell of side 'a'. The inter planar spacing d_{hkl} is given by the relation :

$d_{hkl} = a / \sqrt{(h^2+k^2+l^2)}$

Combining this with Bragg's law, one gets

$\text{Sin}^2 \theta_{hkl} = \lambda^2 *(h^2+k^2+l^2) /4a^2$

The quantity $N = h^2+k^2+l^2$ is an integer. It may be noted that 'N' can not be equal to (8p-1), where p is an integer, i.e. N = 7, 15, 23, 31, 39, 47. All that is necessary to calculate the values of $(\lambda/4a^2)$ and multiply it by the possible values of $N = h^2+k^2+l^2$ to get $\sin^2\theta$ values. The two sets can then be compared to see which of the lines are actually recorded. It may be useful to mention here that values for N for f.c.c. and b.c.c. system are further restricted due to structure factor considerations. Accordingly,

We have simple cubic N= 1, 2, 3, 4, 5, 6, 7, 8, 9, 10, 11, 12, 13, 14, 15, 16, 17, 18, 19, 20, ….. (all hkl)

F.C.C. N= 3, 4, 8, 11, 12, 16, 19, 20, …….(hkl all odd or all even)

B.C.C. N= 2, 4, 6, 8, 10, 12, 14, 16, 18, 20, ……(h+k+l= even)

When the unit cell is unknown, the assignment of indices to various diffraction lines on a powder photograph is tried in order of decreasing symmetry systems. For lower symmetry systems, Ito's method may tried (see Ref. 2).

The characteristic of the cubic system is that values of $\sin^2\theta$ have a common factor ($\lambda/4a^2$). Since tere are three possibilities for structure type in cubic system, one can choose first N values as either 1, 2 or 3 and get the appropriate common factors by dividing the first $\sin^2\theta$ value by these numbers. Others values of $\sin^2\theta$ obtained experimentally are then divided by the common factors just mentioned. The resulting values in case of a correct choice will be close to integers and will correspond to one of the types, simple cubic, f.c.c or b.c.c. Now taking the integer values for the correct/right choice case, one can deduce the common factor for each line by dividing the $\sin^2\theta$ value with the corresponding $N = h^2+k^2+l^2$ value. Since the accuracy of measurements is expected to be better at high Bragg angles (as they correspond to large distances), these only are used to obtained the average value of thee common factor ($\lambda/4a^2$) . By putting the appropriate value of λ for the radiation used, one can determine the lattice parameter 'a'. For determining the unit cell parameter 'a' accurately, the condition can be obtained by differentiating the Bragg's law. This yields

$$\Delta d/d = -\cot\theta\,(\Delta\theta)$$

Since $\cot\theta$ tends to zero as θ approaches 90°, as error Δd in d will reduce to zero. So, accurate cell dimension can be determined from higher Bragg angles and by observing some precaution, viz.,

(a) Coinciding the axis of the Debye Scherrer Camera and the rotation axis of specimen accurately,\
(b) Minimizing the absorption and divergence of the X-ray beam. The error is given by $\frac{1}{2}(\cos^2\theta/\sin^2\theta + \cos^2\theta/\theta)$, and
(c) Accounting for film shrinkage and refraction effects.

The lattice parameter determined from different values of θ are plotted against the error function $\frac{1}{2}(\cos^2\theta/\sin^2\theta + \cos^2\theta/\theta)$, the straight line drawn through the points meets the

Y-axis (corresponding to $\theta = 90°$) and give accurate value of 'a'.

14. Determination of grain size by x-ray line broadening

X-ray powder diffraction lines/rings are expected to be extremely sharp (i.e. δ function or of negligible breadth) if the average grain/crystallite is infinite (or > 1 μm diameter) in size. When the average grain size becomes small i.e. less than 0.1 μm in diameter, diffraction lines/rings exhibit appreciable broadening. If breadth of diffraction line at half of its maximum intensity (or peak height) measured in radians is 'B' at a particular Bragg angle θ (correspondingly at 2θ in the diffractogram Fig. 1), the average grain size (t) of the polycrystalline (or powder) sample is given by the Scherrer relation.

$$t = \frac{0\ \lambda}{B \cos \theta} \qquad \ldots\ldots\ldots\ldots (1)$$

where λ is the wavelength of x-ray beam

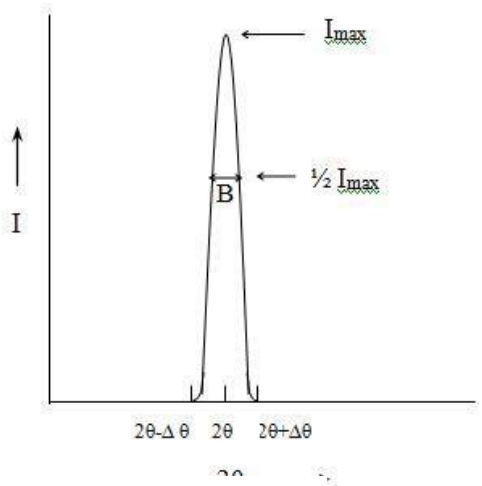

Figure 1

The breadth B in eq. (1) refers to broadening due to grain size alone. It essentially means B is zero when the grain size becomes infinite (i.e. very large). Other factors that lead to additional broadening include incident beam divergence and sample size (in Debye Scherrer Cameras) and width of the x-ray source (in diffractiometers). This is termed as instrumental broadening and present even in samples having grain size exceeding 0.1 – 0.2 μm. It is therefore necessary to make appropriate corrections in the experimentally measured breadths B_m's of diffraction lines determining the true values of 'B' representing only the effect of finite grain size. For this, a diffraction pattern of a standard sample (having particle size > 0.2 μm) is recorded under specified experimental conditions. This contains sharp lines, the breadth (B_s) of each line is measured at half maximum and plotted against the respective angle 2θ to get a correction curve. For doing this, diffraction lines exhibiting K_α doublet are avoided and use is made of K_β line instead. Then the diffraction pattern of the sample under investigation is recorded under identical conditions and breadth of each line (B_m) is

measured again at half of the maximum intensity. Using the B_s versus 2θ plot of standard sample, appropriate value of instrumental broadening is found out for each 2θ angle of diffraction line observed with the given sample. Now If the intensity profile follows a Gaussian distribution The value of 'B' can be determined from

$$B^2 = B_m^2 - B_s^2 \cdots\cdots\cdots\cdots\cdots\cdots\cdots (2)$$

Alternatively for a Cauchy distribution, use can be made of

$$B = \sqrt{B_m^2 - B_s^2} \cdots\cdots\cdots\cdots\cdots\cdots\cdots (3)$$

Once B is known and converted into radians, the average given size (t) can be determined from eq. (1).

It may be mentioned that crystallites possessing internal uniform strains exhibit shift of the diffraction line to other Bragg angles, while those with non-uniform strains depict additional broadening only. Hence, samples are usually subjected to heat treatment to remove strains before recording the diffraction pattern for grain size analysis.

Procedures

1. Record x-ray diffraction pattern of standard powder (size >> 0.2μm) and the given sample under identical conditions by noting them all.
2. Draw correction curve (i.e. B_s versus 2θ) described above from breadth measurements of intensity profile of various reflections of standard.
3. Measure breadth B_m from diffractogram of given sample and record against them the corresponding 2θ angles.
4. Obtain B_s for observed diffraction lines from the B_s versus 2θ graph at appropriate angles.
5. Determine 'B' for each diffraction line using eq. (2) and / or (3) and estimate grain size from eq. (1) by substituting the x-ray wavelength used and the corresponding value of θ.

Report

(a) Grain size as determined from each diffraction line, giving reasons of spread in values, if any.
(b) The spread in the grain size and statistical parameter(s) you can possibly extract from the data.

Questions

1. What are other methods of measuring breadth of intensity profiles? Discuss their relative merits and demerits, if known.
2. Based on experimental findings, suggest which value of grain size can be considered as reasonable and why?
3. Can you suggest a method to isolate line broadening effects caused by non-uniform strains of grains?
4. Estimate breadth 'B' resulting from Yttrium oxide (Y_2O_3) powder of average grain size 100Å using 222, 440, 622 reflections. Y_2O_3 has bcc structure with a = 10.604Å. Assume λ = 2.291Å; Cr K_α.

References

1. B.D. Cullity, Elements of X-Ray Diffraction, Addison-Wisley, Massachusetts (1978)
2. N.F.M. Henry, H. Lipson and W. A. Wooster, The Interpretation of X-Ray Diffraction Photographs, Macmillan, London, (1961).

15. Electron spin resonance (ESR)

Objectives

(i) To observe the ESR signal of Diphenyl Picryl Hydrazyl (DPPH) at radio frequencies and to determine g-factor.

(ii) To determine the full width at half maximum (FWHM) of ESR signals and determine relaxation time.

(iii) To compare the number of spins in given samples of DPPH.

(iv) To measure small magnetic fields by ESR.

Theory

The general field of magnetic resonance involves interactions of magnetic moments with magnetic fields. ESR is the phenomenon involving resonant absorption of energy by systems possessing an unpaired electron (spin). The term resonance implies that the system is in tune with a natural frequency of the magnetic system, which in the present case corresponds to the Larmor frequency of the magnetic moment in the applied magnetic field. The magnetic moment $\vec{\mu}$ is related to the angular momentum $\vec{J}$ by the relation

$$\vec{\mu} = \gamma \vec{J}, \tag{1}$$

where γ is called the gyromagnetic (magnetogyric, more appropriately) ratio. Usually the magnetic moment $\vec{\mu}$ is expressed in terms of a dimensionless quantity g (known as g-factor) and a dimentionless spin angular momentum operator $\vec{S}$ in the following way:

$$\vec{\mu} = g\mu_B \vec{s}, \tag{2}$$

$$\text{and} \quad \vec{J} = \hbar \vec{s}. \tag{3}$$

From Eqs. (1), (2) and (3) it follows that

$$\gamma\hbar = g\mu_B, \tag{4}$$

where μ_B is the Bohr magneton and is sometimes denoted by β. We now begin with the classical description of the motion of $\vec{\mu}$ in an external magnetic field B. We know that $\vec{\mu}$ will precess about $\vec{B}$ with a natural frequency ω given by

$$\omega = \gamma |\vec{B}| . \tag{5}$$

This precession produces an oscillatory magnetic moment in any direction normal to the applied field $\vec{B}$, which can interact with an oscillatory magnetic field $B_1 \cos \omega_1 t$ applied normal to $\vec{B}$. The interaction has a marked effect on the motion of the dipole **( )** $\vec{\mu}$ when ω_1 is close to ω so that we are concerned with a resonance phenomenon. The resonance condition is achieved when

$$\omega_1 = \omega = \gamma |\vec{B}| = \omega_0 \text{ (say)} \tag{5a}$$

and under this condition the component of the dipole along $\vec{B}$ can be altered materially even by very small oscillatory field, i.e., with $B_1 << |\vec{B}|$. So if a circularly p olarized oscillatory magnetic field is applied to the system such that it rotates about $\vec{B}$ in the same sense as $\vec{\mu}$ is doing and is in tune with the Larmor frequency, it causes the dipole to flip down with respect to $\vec{B}$ which corresponds to a higher energy state. This corresponds to an exchange of energy between the oscillatory field and the magnetic system (dipole) (absorption of energy from oscillatory field). It may be noted that a linearly polarized r.f. field can always be decomposed into two circularly polarized components rotating in opposite sense. So one of these components would always be in the correct sense to induce transitions in the magnetic system. That is why in practice a linearly polarized r.f. field is used to observe resonance.

In a simple quantum mechanical description of the phenomenon the interaction of the magnetic dipole $\vec{\mu}$ with $\vec{B}$ and also with a time dependent magnetic field $\vec{B}_1$ (oscillatory) is considered. The Hamiltonian is written as the sum of two terms

$$H = H_o + H_1(t), \tag{6}$$

Where H_o is the steady-state Hamiltonian given by

$$H_o = - \vec{\mu}.\vec{B} = -\mu_B g \, \vec{S}.\vec{B} \tag{7}$$

and $\quad H_1(t) = - \vec{\mu}.\vec{B}_1 = -\mu_B g \, \vec{S}.\vec{B}_1 \cos \omega_1 t.$

The time-dependent term is treated as a small perturbation on the static Hamiltonian H_o. It is well known that an oscillatory perturbation of this type gives rise to a transition probability per unit time (W_{nm}) between states $|\Psi_m\rangle$ and $|\Psi_n\rangle$ given by (see Quantum Mechanics by L.I. Schiff, Chap.8)

$$W_{nm} = \frac{\pi^2}{h^2} g(\upsilon) \left| \langle \psi_m | \; H_1(t) | \psi_n \rangle \right|^2$$

$$= \frac{\pi^2 \mu_B^2}{h^2} g(\upsilon) \left| \langle \psi_m | g \vec{S}.\vec{B}_1 | \psi_n \rangle \right|^2 , \qquad (9)$$

where $|\Psi_m>$ and $|\Psi_n>$ are the eigenfunctions of the static Hamiltonian H_o appropriate to the energies E_m and E_n ($E_m > E_n$). $g(\nu)$ is called the line shape function and is usually Lorentzian. The maximum power absorbed per unit volume (i.e. at the centre of the resonance line) is given by

$$P_{ab} = W_{nm} N (E_m - E_n) , \qquad (10)$$

where N is the effective number of spins taking part in a resonance absorption and is equal to the population difference between the two levels concerned. Eq. (10) determines the conditions for a resonance experiment. For a situation where N = 0 the magnetic system is said to be saturated as the system can absorb no more power. Normally saturation should be avoided since it reduces the resonance signal and also distorts the line shapes. In addition W_{mn} will be large only when Bohr frequency condition is satisfied, i.e.,

$$E_m - E_n = h\nu_o , \qquad (11)$$

where $\nu_o = \omega_o/2\pi$ is the resonance frequency. The other term which contributes to W_{nm} is $\langle \psi_m | g S.B_1 | \psi_n \rangle$ and this is what provides the selection rules for a given transition and the condition that, $\vec{B}_1$ should be normal to $\vec{B}$. For the simple case of single unpaired electron (spin) the resonance condition is shown in Fig. 1 below.

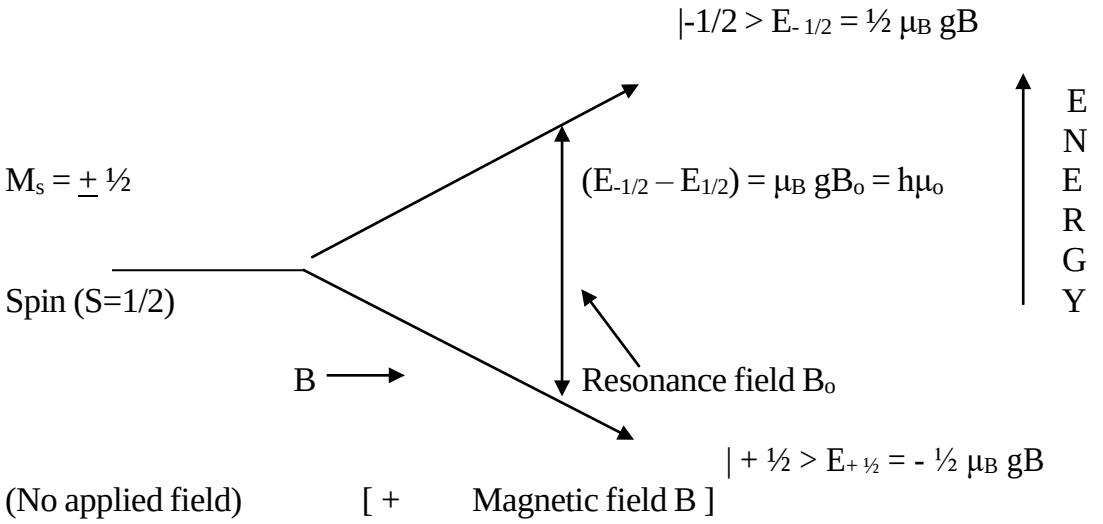

Fig. 1. Splitting of ± ½ states in an applied magnetic field B.

Hence the resonance condition is given by

$$h\nu_o = g\ \mu_B B_o\ . \tag{12}$$

Using Eqs. (4) and (5) we can rewrite Eq. (12) as

$$\omega_o = 2\pi\nu_o = \gamma B_o. \tag{13}$$

Spin-lattice and spin-spin relaxation times

What happens to the excited spin under the resonance condition? There exists a coupling between the magnetic system (frequently referred to as the "spin-system") and the crystal lattice containing the "spin-system", which provides an alternative path by means of which excited spins may return to the lower level by some non-radiative process. This is called the "Spin-Lattice-Relaxation". The line width of resonance $(\Delta\nu_{SL})$ due to spin-lattice relaxation is approximately given by

$$(\Delta\nu_{SL}) = \frac{1}{T_1}\ , \tag{14}$$

where T_1 is known as the Spin-Lattice Relaxation Time. T_1 is the life time by which the spin-lattice relaxation is being characterized. In addition the interaction between similar magnetic species (i.e, spins) is another source of line broadening. This interaction is termed as spin-spin relaxation and is characterised by a life time T_2. The line width $(\Delta\nu_{SS})$ due to spin-spin interaction is given by

$$(\Delta\nu_{SS}) = \frac{1}{T_2}\ . \tag{15}$$

While it is usual to study T_1 and T_2, due to limitations we shall concern ourselves with the total relaxation time $T = 2/\Delta\nu$, where $\Delta\nu$ is the full width at half maximum (FWHM) of the ESR signal.

III Experimental set-up

One of the simplest ways of observing ESR is by incorporating the sample in a coil of a tuned circuit, so that it controls the inductance of the coil. Then under conditions of resonance, the radio frequency (r.f.) power absorbed by the coil will be at its maximum so that we measure a decrease in amplitude of rf- oscillations. Resonance can be detected by sweeping the resonance magnetic field by means of an extra pair of coils (Helmholtz Coils driven by 50 Hz a.c. current) called the sweep coils. At r.f. we need very small magnetic fields to observe ESR (estimate resonance field for an electron at 10 MHz), therefore the r.f. experiment is performed in zero externally applied DC field .The desired resonance field is generated by means of sweep coils only.

(Notice the time scales of the magnetic field sweep and the precession of the spin.) However, if we desire to perform ESR at microwave frequencies (X-band frequencies 10^{10} Hz) or a similar nuclear magnetic resonance (NMR) experiment at r.f. for a proton at 10

MHz, electromagnets are required to apply the desired DC magnetic field for resonance. The set-up used here is shown in Fig. 2 and its block diagram is shown in Fig. 3.

IV Operation

Familiarize yourself with all the knobs and their functions before actually starting the experiment. Place the sample tube in the sample coil gently* and proceed as follows:

(1) Connect the X and Y terminals to the corresponding terminals of CRO by connecting leads.

(2) Connect the Helmholtz coil-leads to terminals marked as 'H-coils'.

(3) Adjust the `current' knob fully anti-clockwise (minimum).

(4) Adjust the `phase' knob to centered position.

(5) Adjust the `sensitivity' knob fully clockwise (maximum).

(6) Adjust the `Frequency' knob fully clockwise (maximum).

(7) Connect the ESR unit and CRO to A.C. mains and turn the `mains' switch `ON'.

(8) Adjust the X-deflection of CRO to almost full scale and Y-amplifier gain to about 0.2 V/cm.

(9) Now turn the `H-coils' switch `ON' and rotate the current knob slowly for about 150 mA current in the milliammeter.

You will observe the resonance peaks on CRO. Now adjust the `phase' knob to coincide two peaks over the other two and adjust the horizontal and vertical gains of CRO and `sensitivity' knob for a proper display. Place the pick-up coil connected to the digital frequency counter near the sample coil to measure the resonance frequency.

V Measurements

(i) Resonance field

Let the horizontal deflection be set for p(mm) end to end and the separation between the two peaks be Q(mm) (see Fig. 2) for a given current I (ma, rms value) in H-coils. Then the resonance field B_o in gauss is given by

---

*You may find the sample permanently fixed in the sample coil. In that case do not fiddle with it.

$$B_o = \frac{1}{2} K I Q/p, \qquad (16)$$

where K is a constant which depends on the number of turns and radius of the Helmholtz coils. For the present set-up K =156x10^{-3}. From Eq. (12) calculate g-factor after knowing B_o and ν_o (as measured by frequency counter). Calculate B_o for several values of I between 100mA and 250mA (at least 10 settings) and from corresponding values of Q. To measure Q more precisely the peaks are made to cross near the base line P_1P_2 at points Q_1 and Q_2 by properly adjusting the phase and the signal height (Fig. 2). Now mark the points P_1, P_2, Q_1 and Q_2 on a tracing paper and measure P and Q with the help of a mm scale. Make several attempts for the measurement of Q and P. Determine an average value of Q/P. Find the average value of g-factor. Now change the frequency by adjusting the `frequency' knob to a new position and repeat the above measurements for the new frequency set. Perform the experiment for at least five sets of frequency.

(ii) a. <u>Line width of signal</u>

Take trace of ESR signal on a transparent piece of paper from the CRO screen. The signal height may be maximized to full vertical scale of the screen. The current values should be kept between 100 and 150mA for better accuracy. Measure the full width at half maximum (FWHM) in mm from the trace. Make several observations for different currents and frequencies. Repeat the measurements with different samples of DPPH given to you. You will notice different line widths. As an exercise you can dissolve DPPH in different solvents (e.g. chloroform, benzene or acetone) to see the effect on the line width. Samples recrystallized from acetone solution give narrower signals while samples recrystallized from benzene give wider signals. Also older DPPH samples give a wider ESR signals. Line width in mm may now be converted either in magnetic field units (gauss) or in frequency units(Hz). To obtain FWHM ΔB in gauss from FWHM Δx in mm, we use the relation

$$\Delta B = \frac{KI\,\Delta x}{p} \quad . \qquad (17)$$

To convert the line width Δx in units of Hz we need to calibrate the horizontal (X-deflection) scale in unit of Hz/mm. To do this we observe the shifts in the resonance peaks for a given current by changing frequency from ν_{max} to ν_{min} with the help of 'frequency' knob. Let δx be the average shift in the resonance peaks in mm, then the horizontal scale is equal to $(\nu_{max} - \nu_{min})/\delta x$ (Hz/mm). δx is measured with the help of the corresponding peak separations Q_{max} and Q_{min} using the following relation:

$$2\delta x = Q_{max} - Q_{min},$$

where Q_{max} and Q_{min} refer to the peak separation Q corresponding to ν_{max} and ν_{min}, respectively.

To get the FWHM $\Delta\nu$ in Hz we use the relation

$$\Delta\nu = 2\,\frac{(\nu_{max} - \nu_{min})\Delta x}{Q_{max} - Q_{min}} \quad . \tag{18}$$

From the measured FWHM $\Delta\nu$ we can determine the relaxation time by using the relation

$$T = \frac{2}{\Delta\nu} \quad . \tag{19}$$

(ii) b <u>Line shape of ESR Signal</u>

The DPPH line is an exchange narrowed line and exhibits a Lorentzian shape which may be described by

$$Y = Y_o\,\Delta^2/\{\Delta^2 + (B-B_o)^2\}, \tag{20}$$

where Δ is the half width at half maximum (HWHM).

With the measured value of ($\Delta B = 2\Delta$), see if the above equation is a good description of the line shape observed by plotting Y as a function of B around $\mathbf{B_0}$.
Epression (20) may be expressed in terms of x-axis divisions instead of magnetic field units as

$$Y = Y_0\,(\Delta x)^2/[(\Delta x)^2 + 4(x-x_0)^2] \tag{21}$$

Where Δx is the FWHM in x-axis divisions, x_0 is the centre of peak ,Y_0 is the peak height at x_0, and x is an arbitrary position on x-axis .The origin is where B=0 i.e. the mid point between the two peaks. Alternatively, the origin may be assigned to the centre of the peak ie at x_0 and we may express (21) in terns of $X=(x-x_0)$ as

$$Y(X) = Y_0\,(\Delta x)^2 / [(\Delta x)^2 + 4\,X^2] \tag{22}$$

Plot experimental vaules of Y and calculated values of Y vs. X and comment on the fit.

(iii) Comparison of number of spins in given samples

As the intensity of the absorption signal is proportional to the area between the base line and the ESR signal, the integrated intensity I (under no saturation conditions) may be expressed as

$$I \quad \alpha \quad \text{Total number of spins.}$$

If we compare integrated intensities for two given samples under identical experimental conditions, we get the ratio of the number of spins in the two given samples as

$$I_1/I_2 = N1/N2 . \tag{23}$$

If one of the samples has known number of spins then one can determine the number of spins in the unknown one. You may prepare several different samples of DPPH for this part.

(iv) Measurement of small magnetic fields

When a small magnetic field is applied to the sample by means of bar magnet(s) along the axis of the Helmholtz coils the resonance peaks shift in proportion to the additional magnetic field from their initial positions. The shift in mm may be converted in units of gauss by relation (17) to calculate the field due to the bar magnet(s) at the sample. Place the bar magnet(s) along the axis of the Helmholtz coils at different distances and measure the magnetic field due to the bar magnet(s) at the sample. Plot a graph showing the variation with distance.

VI Questions

1. What are the basic differences between an r.f. and a microwave frequency ESR experimental set-up? Explain, the main modifications required in the present set-up to observe ESR at 3 cm wavelength.

2. The FWHM of DPPH ESR signal is expected to be on the order of 30 gauss. But the observed line width is much smaller (~ 3 gauss). Can you find out the reasons?

3. The line position and the line width are two useful parameters of an ESR measurement. What informations do these parameters provide about the sample ?

4. For the simple case of spin 1/2 system show that only $\vec{B}_1 \perp \vec{B}$ gives a resonance signal. Make use of Eq.(10) to show this.

5. ESR and NMR can in principle be used to measure magnetic fields. Which of the two is practically used for such measurements and why ?

6. With the help of a diagram, show how many resonance signals will be there for S = 1/2 and the nuclear spin I = 3/2 system.[Make use of the selection rule: $\Delta M_S = \pm 1$ and $\Delta M_I = 0$, where M_S and M_I represent the corresponding spin quantum numbers.]

VII References

1. E. Zavoiski, J. Phys. USSR 9, 211(1945) (for the discovery of ESR).

2. C. Kittel,`Introduction to Solid State Physics', Vth Ed., Chap.16.

3. C.P. Poole Jr., 'Electron Spin Resonance', Chs. 1 & 2.

4. W.T. Dixon, 'Theory and Interpretation of Magnetic Resonance Spectra'.

5. G.E. Pake, Am. J.Phys **10**, 438 and 473 (1950) and in 'Paramagentic Resonance'.

6. C.P. Slichter, 'Principles of Magnetic Resonance', Chs. 1 & 2.

7. D.J.E.Ingram, 'Spectroscopy at Radio and Microwave Frequencies', 2nd Ed. (1967).

8. D.J.E. Ingram, 'Free Radicals as Studied by ESR', Chs. 1 & 2.

9. Willard, Meritt, Dean & Settle, `Instrumental Methods of Analysis', 6th Edition, Chap. 12.

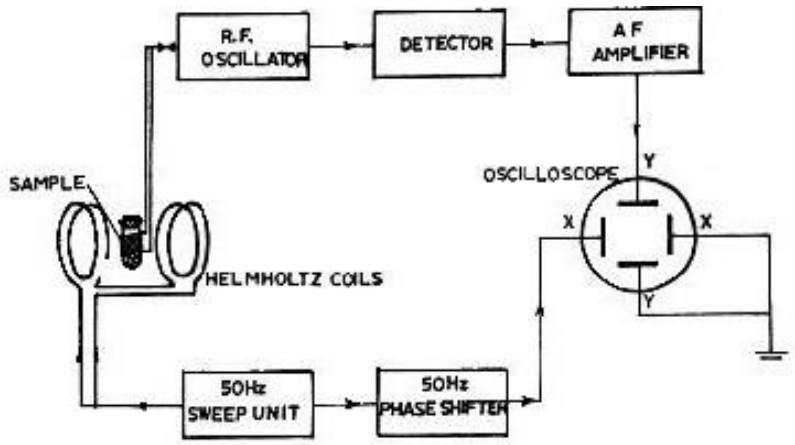

Fig. 3 Block diagram of the ESR set up

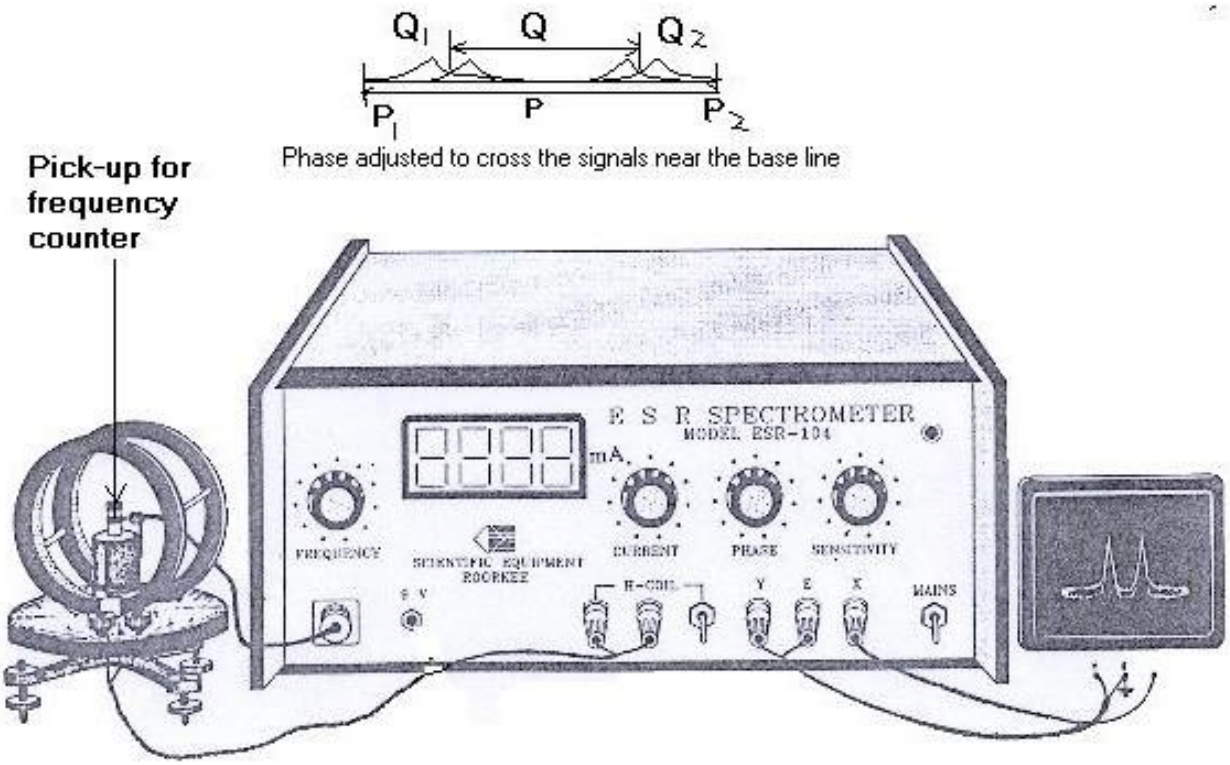

Fig. 2 Experimental set up for ESR

16) Objective: To Study of Hysteresis Loop of Ferromagnetic Materials

INTRODUCTION

A precise knowledge of various magnetic parameters of ferromagnetic substances and the ability to determine them accurately are important aspects of magnetic studies. These not only have academic significance but are also indispensable for both the manufacturers and users of magnetic materials.

The characteristics which are usually used to define the quality of the substance are coercivity, retentivity, saturation magnetisation and hysteresis loss. Furthermore, the understanding of the behavior of these substances and improvement in their quality demand that the number of magnetic phases present in a system is also known. The information about the aforementioned properties can be obtained from a magnetisation hysteresis loop which can be traced by a number of methods in addition to the slow and laborious ballistic galvanometer method. Among the typical representatives of AC hysteresis loop tracers some require the ring form of samples, while others can be used with thin films, wires or even rock and mineral samples. Toroidal or ring form samples are more convenient because of the absence of demagnetising effect due to closed magnetic circuits, but are not practicable to make all test samples in toroidal form with no free ends. Further every time the pickup and magnetising coils has to be wounded on them and hence are quite inconvenient and time consuming. In the case of open circuit samples, the free end polarities gives rise to demagnetising field which reduces the local field acting in the specimen and also makes the surrounding field non-uniform. Therefore, it becomes necessary to account for this effect lest the hysteresis loop is sheared. In case of conducting ferromagnetism, several additional problems arise due to eddy currents originating from the periodic changes in applied magnetic field. These currents give rise to a magnetic field in the sample which counteracts the variation of the external field and, in turn, renders the field acting in it non uniform and different from the applied field, both in magnitude and phase. Thus apart from resistive heating of the samples, because of the eddy currents the forward and backward paths traced near saturation will be different, which will lead to a small loop instead of a horizontal line in the magnetic polarisation (J) against field (H) plot Fig. 1. The intercept of the magnetic polarization axis, which corresponds to retentivity and saturation magnetic polarization tip will continue to increase with applied field up to very high values. Accordingly, retentivity (Jr) and saturation magnetic polarization (Js) will be asymptotic values of the J-intercept and tip height respectively against H plots. Furthermore, the width of the loop along the direction of the applied field will depend on its magnitude and will continue to increase because shielding due to eddy currents is proportional to the external field. Therefore, the true value to coercivity (JHc) corresponding to no eddy currents situation, will be obtained by extrapolating the half loop width against field line to the H=0 axis. Obviously the effect of eddy currents will be more pronounced in thicker samples than in thin ones.

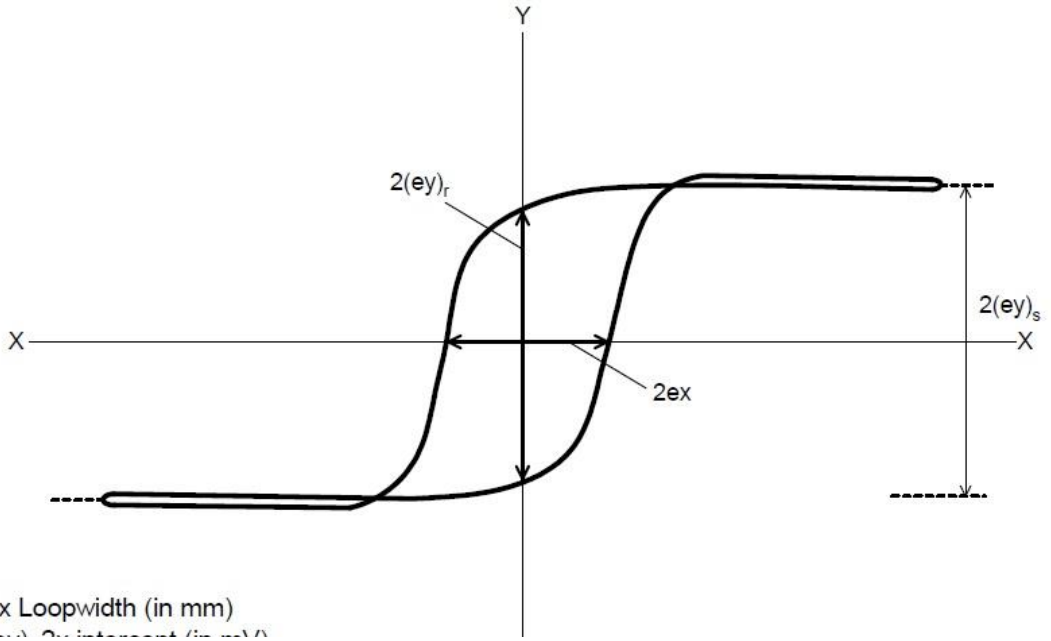

2ex Loopwidth (in mm)

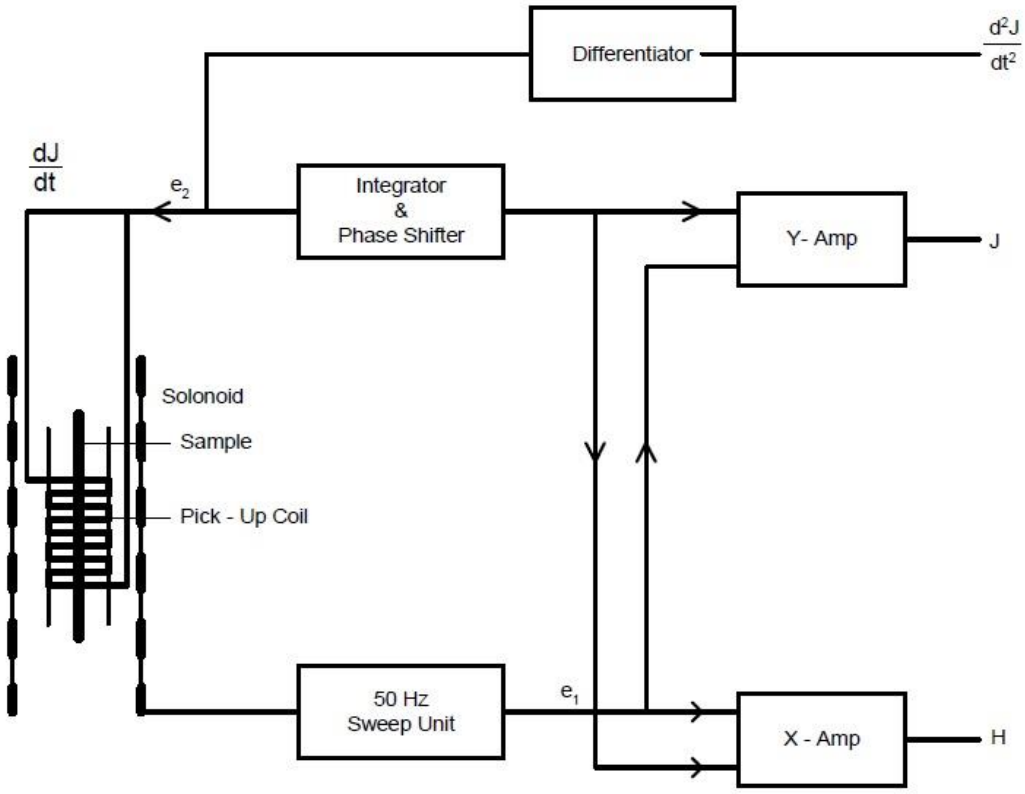

Fig. 2: Block Diagram of Hysteresis Loop Tracer

DESIGN PRINCIPLE

When a cylindrical sample is placed coaxially in a periodically varying magnetic field (say by the solenoid) Fig. 2 the magnetisation in the sample also undergoes a periodic variation. This variation can be picked up by a pickup coil which is placed coaxially with the sample. Normally, the pickup coil is wound near the central part of the sample so that the demagnetisation factors involved are ballistic rather than the magneto metric.

For the uniform field H_a produced, the effective field H acting in the cylindrical sample will be

$H = H_a - NM$ where M is the magnetisation, or

$$H = H_a - \frac{NJ}{\mu 0} \qquad (1)$$

Where N is the normalised demagnetisation factor including 4π and J is the magnetic polarization defined by

$$B = \mu_0 H + J \qquad (2)$$

With $B=\mu H$ or $\mu_0 (H+M)$ as magnetic induction. The signal corresponding to the applied field, Ha, can be written as

$$e_1 = C_1 H_a \qquad (3)$$

Where C_1 is a constant.

Further the flux linked with the pickup coil of area A_c due to sample of area A_s will be

$$\phi = \mu_0 (A_c - A_s) H' + A_s B$$

Here H' is the magnetic field, in the free from sample area of the pickup coil, will be different from H and the difference will be determined by the magnitude of demagnetising field. However, when the ratio of length of the sample rod to the diameter of the pickup coil is more than 10, the difference between H and H' is too small, so that $\phi = \mu_0(A_c - A_s)H' + A_s B$

$$= \mu_0 A_c H + A_s (B - \mu_0 H)$$

$$\Rightarrow \phi = \mu_0 A_c H + A_s J \qquad (4)$$

The signal e_2 induced in the pickup coil will be proportional to $\frac{d\emptyset}{dt}$

After integration the signal (e_3) will, therefore be

$$e_3 = C_3\phi = C_3\mu_0 A_c H + C_3 A_s J \qquad (5)$$

Solving equations (1), (3) and (5) for J and H give

$$C_1 C_3 A_C \left(\frac{A_s}{A_c} - N\right) J = C_1 e_3 - \mu_0 C_3 A_C e_1 \qquad (6)$$

And $C_1C_3A_C\left(\frac{A_s}{A_c}-N\right)H = C_3A_se_1 - \frac{N\,C_1e_3}{\mu_0}$ (7)

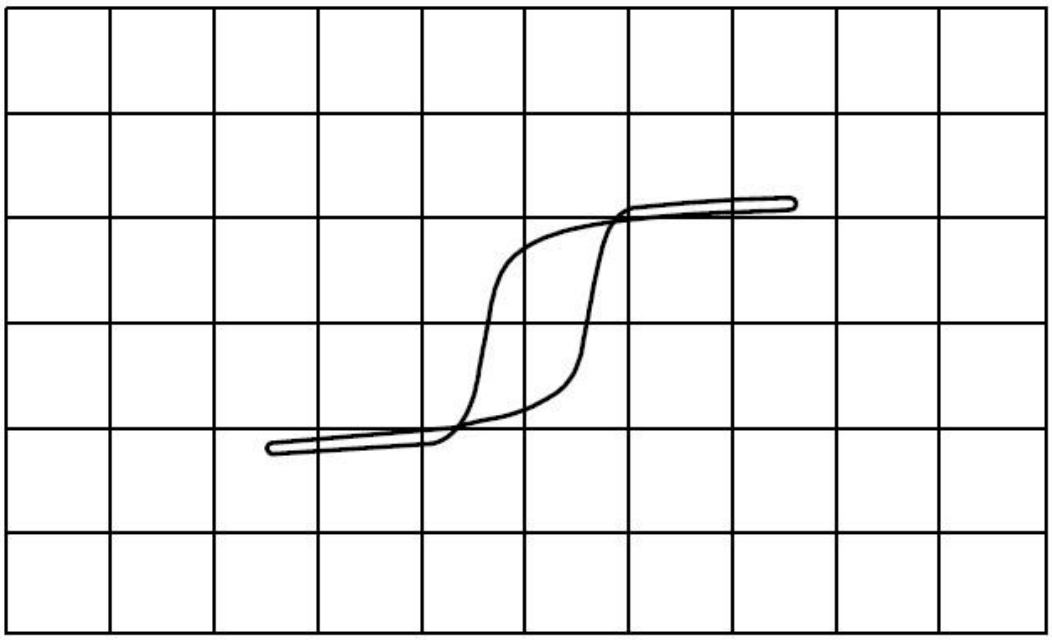

Fig. 3 (a) : J-H Loop

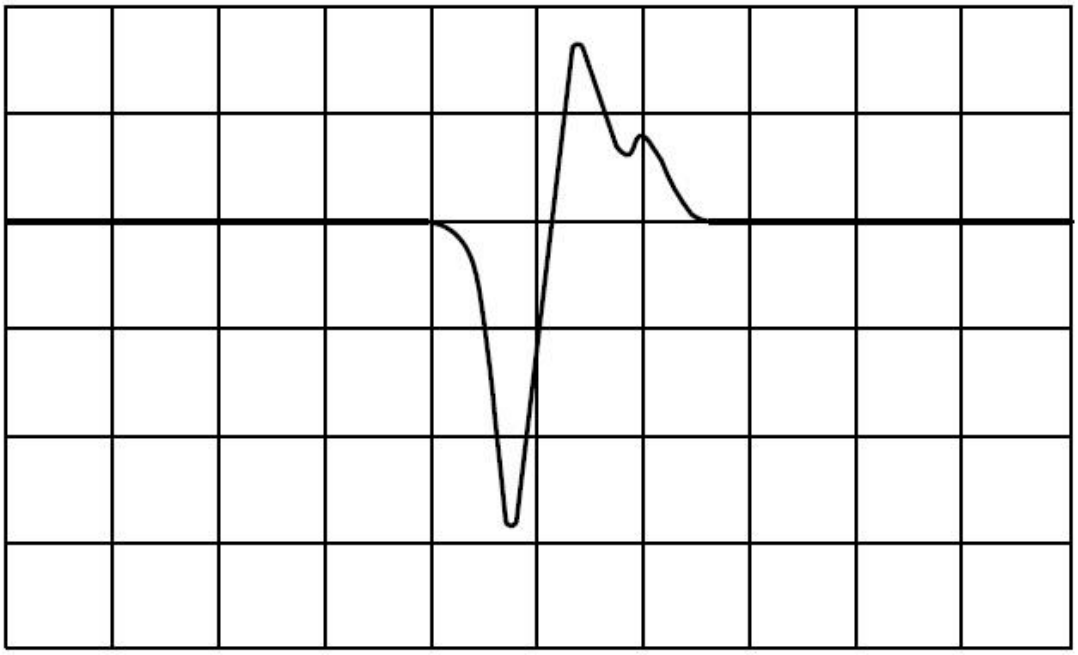

Fig. 3 (b) : $\frac{d^2J}{dt^2}$ Showing Two Magnetic Phase

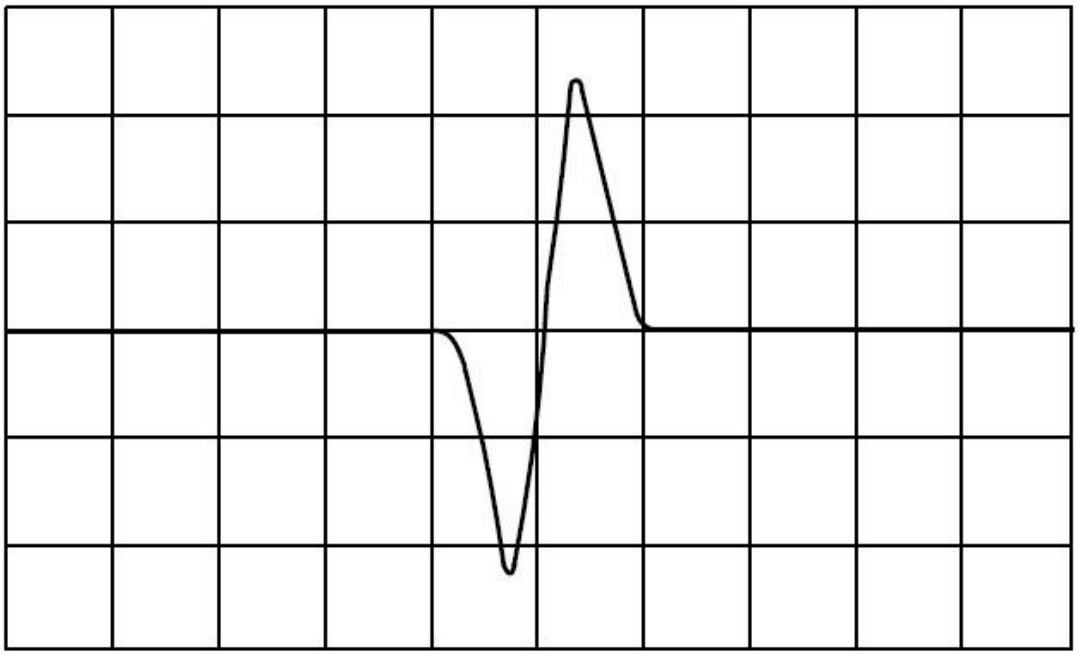

Fig. 3 (c) : $\frac{d^2J}{dt^2}$ Showing a Single Magnetic Phase in The Sample

Based on these equations an electronic circuit may be designed to give the values of J and Hand hence the hysteresis loop.

In case the sample contains a number of magnetically different constituents, the loop obtained will be the algebraic sum of individual loops of different phases. The separation of these is not easy in a J-H loop while in a second derivative of J, $\frac{d^2J}{dt^2}$, the identification can be made very clear.

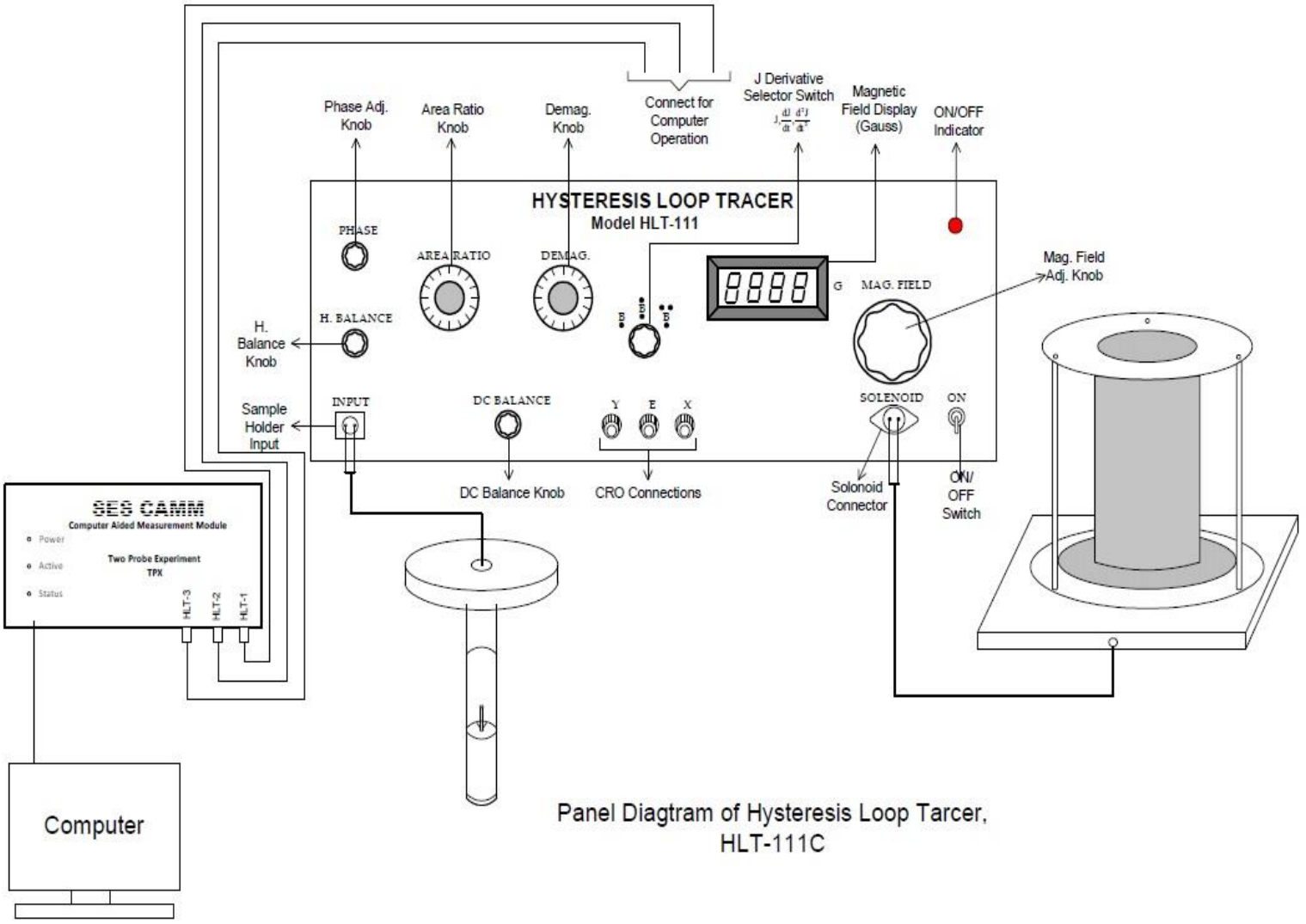

Panel Diagtram of Hysteresis Loop Tarcer, HLT-111C

Laboratory setup

(HLT-111C)

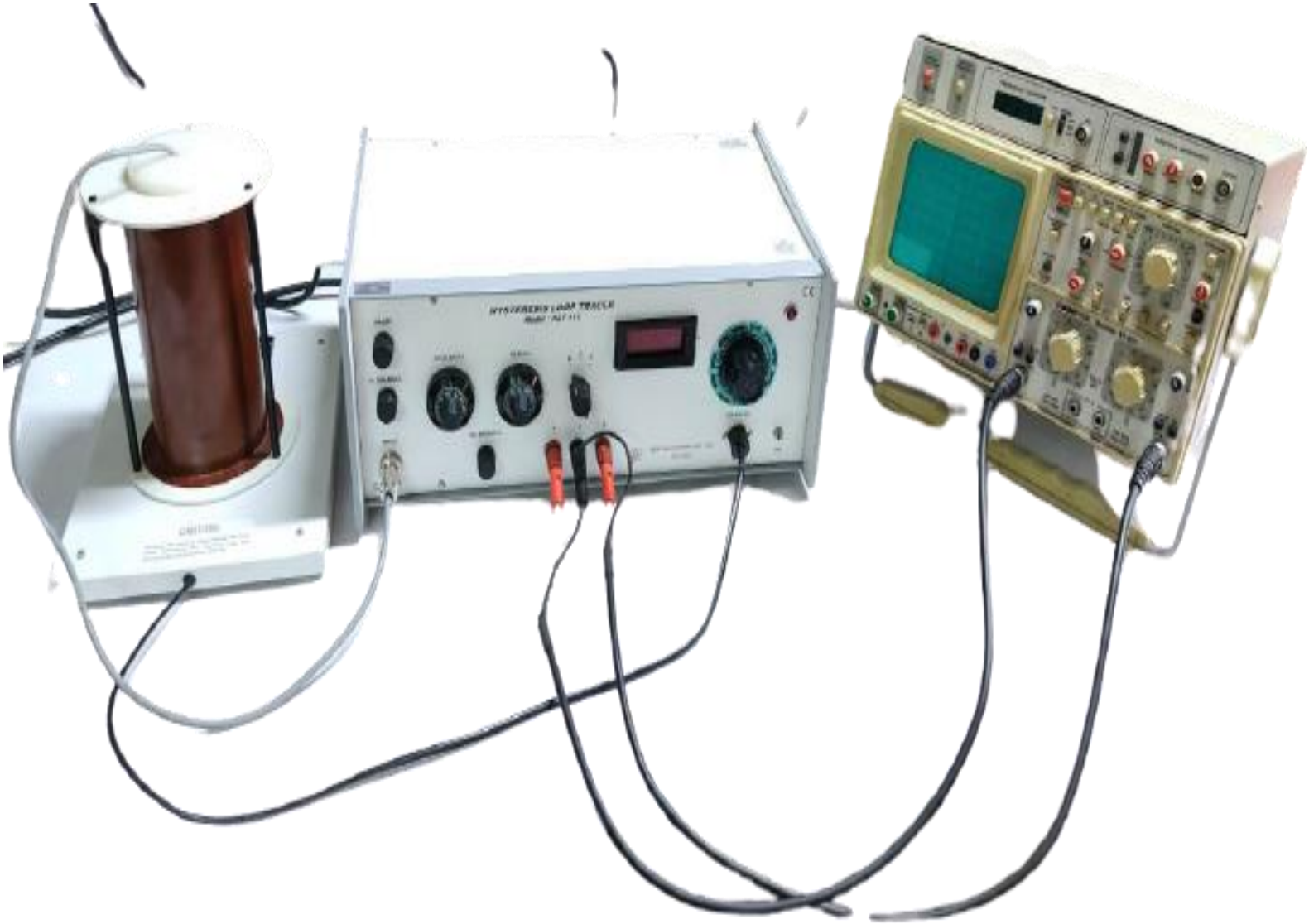

1) Power Supply Unit

2) Sample Holder

3) CRO

4) Solenoid

Different parts of Hysteresis Loop Tracer (HLT-111C)

OBSERVATIONS & TABULATIONS

For this instrument diameter of pickup coil= 3.26 mm

g_x = 100 & g_y = 1

Sample: Commercial Nickel (Standard)

Length of sample = 37 mm

Diameter of sample = 1.20 mm

Magnetic Field = 200 gauss

Therefore, area ratio $\left(\frac{A_s}{A_c}\right)$ = 0.135

Demagnetisation factor (N) = 0.0033 (for C/a = 30.8 from table)

Calibration

Without sample, Oscilloscope at D.C. Time base EXT, H Bal, Phase and DC Balance adjusted for horizontal straight line in the center. Demagnetisation at zero and Area ratio 0.40* at magnetic field (H_a) 200 gauss (rms).

e_x = 6.2 mm or

= 6.4 V (if read by applying on Y input of CRO)

For area ratio of unity e_x = $\frac{62}{0.40}$ = 155 mm ⇒ 16 V

As we know, $G_O = \frac{H_a}{e_x}$, So,

G_O (rms) = $\frac{200}{155}$ = 1.29 gauss/mm

G_O (Peak to Peak) = 1.29 x $2\sqrt{2}$ = 3.64 gauss/mm

Also,

G_O (rms) $= \frac{200}{16} = 12.5$ gauss/volt

G_O (Peak to Peak) $= 12.5 \times 2\sqrt{2} = 35.25$ gauss/volt

Adjustment

By adjusting N and (A_S/A_C) as given above the J-H loop with is too small. Thus both are adjusted to three** times i.e. 0.405 and 0.0099 (Full value of area ratio pot = 1.000. Full value of demagnetisation pot = 0.100) respectively.

**Any other factor of area ratio may also be chosen, if the x-gain of the CRO is not sufficient. Observed value of e_x should then be divided by the other factor to obtain e_x for unity area ratio.*

***Or any other factor so that a good J-H loop of width (=20 mm) is observed. Please remember to divide by this factor in calculating pf the loop width.*

EXPERIMENTAL PROCEDURE

1. Before Turning ON the power supply, check all the connections are properly connected or not. Then set **AREA RATIO** nob to 4 (=0.40) and **DEMAG.** nob to 0 as shown below:

2. Now Turn ON power supply of main unit and CRO. Set CRO screen with a dot at origin and then set magnetic field to 200 gauss using Solenoid nob as shown below:

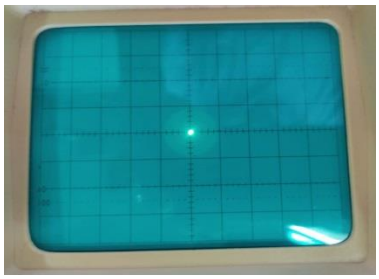

3. After setting magnetic field to 200 gauss, you will find a random image on CRO screen. Now make it a straight line over x-axis using Phase , H. Balance, DC Balance nob of main unit and Left-Right nob of CRO as shown below:

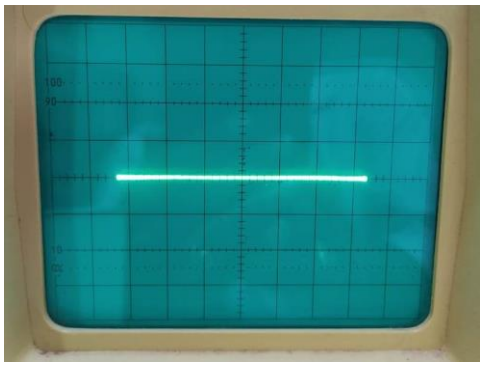

4. Now set **AREA RATIO** nob to 405 (=0.405) and **DEMAG.** nob closed to 1 as shown below:

5. Now pull out the sample holder from coil segment, place the desired sample (like comm. Nickel) in sample holder and put in the sample holder inside the coil segment again as shown:

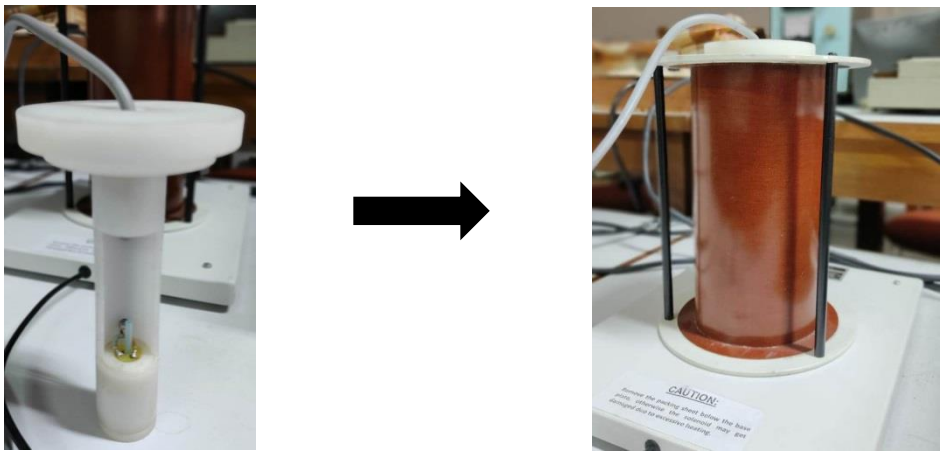

6. Now you can see a Hysteresis Loop of comm. Nickel sample. Then using Phase , H. Balance, DC Balance nob of main unit, make it more refine as shown below:

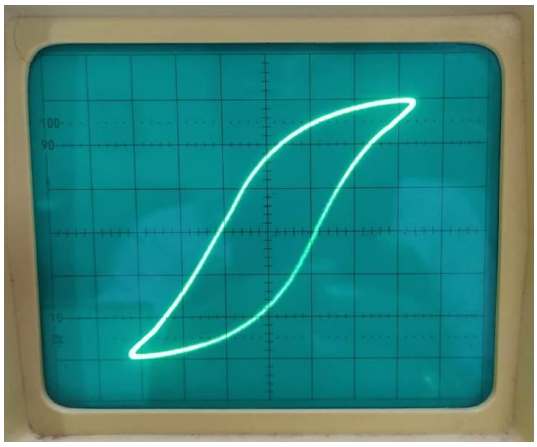

7. Now this process is successfully completed.

For (sample name)				
		Coercivity	**Saturation Magnatisation**	**Retentivity**
S. No.	**Mag. Field (Gauss)**	**Loop width (mm)***	**Tip to Tip hight (mV)***	**Intercept (mV)***
1	25			
2	50			
3	75			
4	100			
5	125			

6	150			
7	175			
8	200			
9	225			
10	250			
11	275			

8. Now make a tables as shown below and start filling your observations and calculations for the different magnetic fields:

*****_For the parameter mentioned in the table, refer to fig. 1._

9. Now Plot graphs for ***Coercivity Vs Mag. Field***, ***Saturation Magnatisation Vs Mag. Field*** and ***Retentivity Vs Mag. Field.***